Supporting Information for

Modulation of Fluorescent Protein Chromophores to Detect Protein Aggregation with Turn-on Fluorescence

Yu Liu[1], Charles H. Wolstenholme[1], Gregory C. Carter[3], Hongbin Liu[2], Hang Hu[2], Leeann S. Grainger[1], Kun Miao[1], Matthew Fares[1], Conner A. Hoelzel[1], Hemant P. Yennawar[3], Gang Ning[4], Manyu Du[3], Lu Bai[3], Xiaosong Li[2], Xin Zhang[1, 3, 4*]

[1]Department of Chemistry, [3]Department of Biochemistry and Molecular Biology, [4]The Huck Institute of Life Sciences, The Pennsylvania State University, University Park, Pennsylvania, 16802, United States.

[2]Department of Chemistry, University of Washington, Seattle, WA 98105, United States.

*Correspondence should be addressed to Xin Zhang (xuz31@psu.edu).

Table of Contents

Note S1: Fluorescence of probes are insensitive to pH. Fluorescence emission can be sensitive to pH values. This sensitivity is important to understand for better biological applications. For example, lysosome is an acidic cellular compartment that has a pH value near 4.5. To determine whether fluorescence of probes studied in this work is sensitive to pH, we measured fluorescence excitation and emission spectra in solvents with varying pH values. The pH value of glycerol solution in our measurement is ~ 6.0, therefore a 90% glycerol and 10% water mixture resulted in a pH 6.0 solution. The basic solution was produced by a mixture of 90% glycerol and 100 mM Tris•HCl at pH 8.5. The acidic solution was produced by a mixture of 90% glycerol and 300 mM NaOAc•HCl at pH 4.5, a pH value that is normally found in lysosome. Finally, a near neutral solution at pH 7.5 was produced by a mixture of 90% glycerol in PBS buffer. Thus, these solutions collectively give us the measurement of pH values at 4.5, 6.0, 7.5, and 8.5. The pH sensitivity of HBI is expected due to the pKa of the phenol group at ~8.5, and our experiment confirmed this notion (Figure S5). All other probes were insensitive to pH values and exhibited almost identical excitation and emission spectra (Figures S6-10).

Note S2: Fluorescence of 3 originated from α-synuclein fibers. We demonstrated that fluorescence of **3** originated from α-synuclein fibers. In this experiment, 140 μM of α-synuclein were incubated with varying concentrations (1, 2.5, 5, 10, 20 μM) of probe **3**. Aggregation of α-synuclein was induced by incubating the protein samples at 37 ºC with 1,350 rpm shaking on an orbital shaker for 72 h. Mature fiber formation was confirmed by TEM (Figure S13a) and fluorescence of probe **3** was measured using a fluorescence microplate reader. We found that the fluorescence of probe **3** was positively proportional to its concentration, suggesting that all of the probe **3** bound to α-synuclein fibers and emitted fluorescence quantitatively. As a comparison, similar observations were made using ThT under the identical experimental condition.

Note S3: Fluorescence signal is stoichiometric towards protein aggregates. A general and critical concern for any fluorescence-based assay is whether the signal is stoichiometric to the total amount of the targeted analytes. The stoichiometry is important for an assay to accurately report on the concentration of an analyte. In our case, in order to reliably report on the amount of protein aggregates in live cells and the aggregation kinetics in buffer, the fluorescence signal needs to be stoichiometric towards the total amount of protein aggregates. We demonstrate such a property using SOD1-V31A (Figure S15c). In this experiment, 20 μM of **3** was incubated with varying concentrations (1, 2.5, 5, 10 μM) of purified SOD1-V31A. Aggregation of SOD1-V31A was induced by incubating the protein samples at 59 ºC for 30 min in the presence of 83 mM EDTA. We found that the fluorescence of probe **3** was proportional to the concentration of SOD1-V31A, suggesting that the fluorescence intensity quantitatively reports on the amount of protein aggregates.

Note S4: Non-fluorogenic approaches to visualize protein aggregation in live cells. When HEK293T cells expressed either Htt-97Q-mCherry or Htt-97Q-Halo conjugated with an always-fluorescent TMR ligand, we identified obvious fluorescent punctate structures with diffuse background fluorescence (Figure S18b). Cells expressing the non-aggregating Htt-0Q-Halo in conjugation with TMR exhibited only diffuse fluorescence (Figure S18b). Thus, protein aggregation is primarily judged by the appearance of fluorescent puncta in non-fluorogenic methods (Figure S18a)

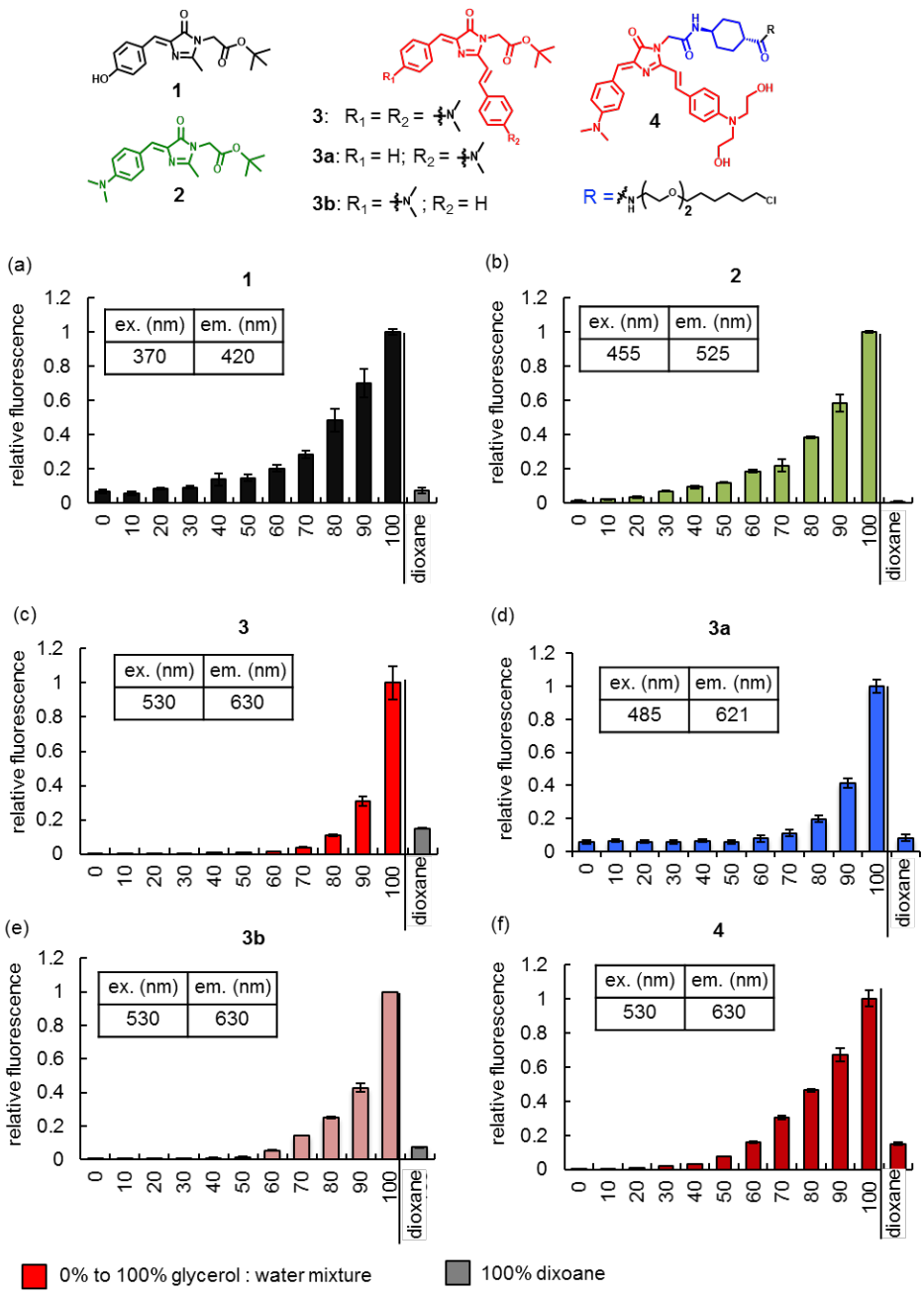

Figure S1: Fluorescence response of FP chromophore analogues in H_2O with increasing concentrations of glycerol. FP analogues (20 µM) were prepared in glycerol:H_2O mixture with increasing glycerol concentrations. In addition, fluorescence intensity in 1,4-dioxane was measured to evaluate their response to polarity. Fluorescence measurement was carried out using a Tecan infinite M1000Pro fluorescence microplate reader at excitation and emission wavelengths as indicated. All readings were normalized against the fluorescence intensity in 100% glycerol as 1. Error bars: standard error (n=3).

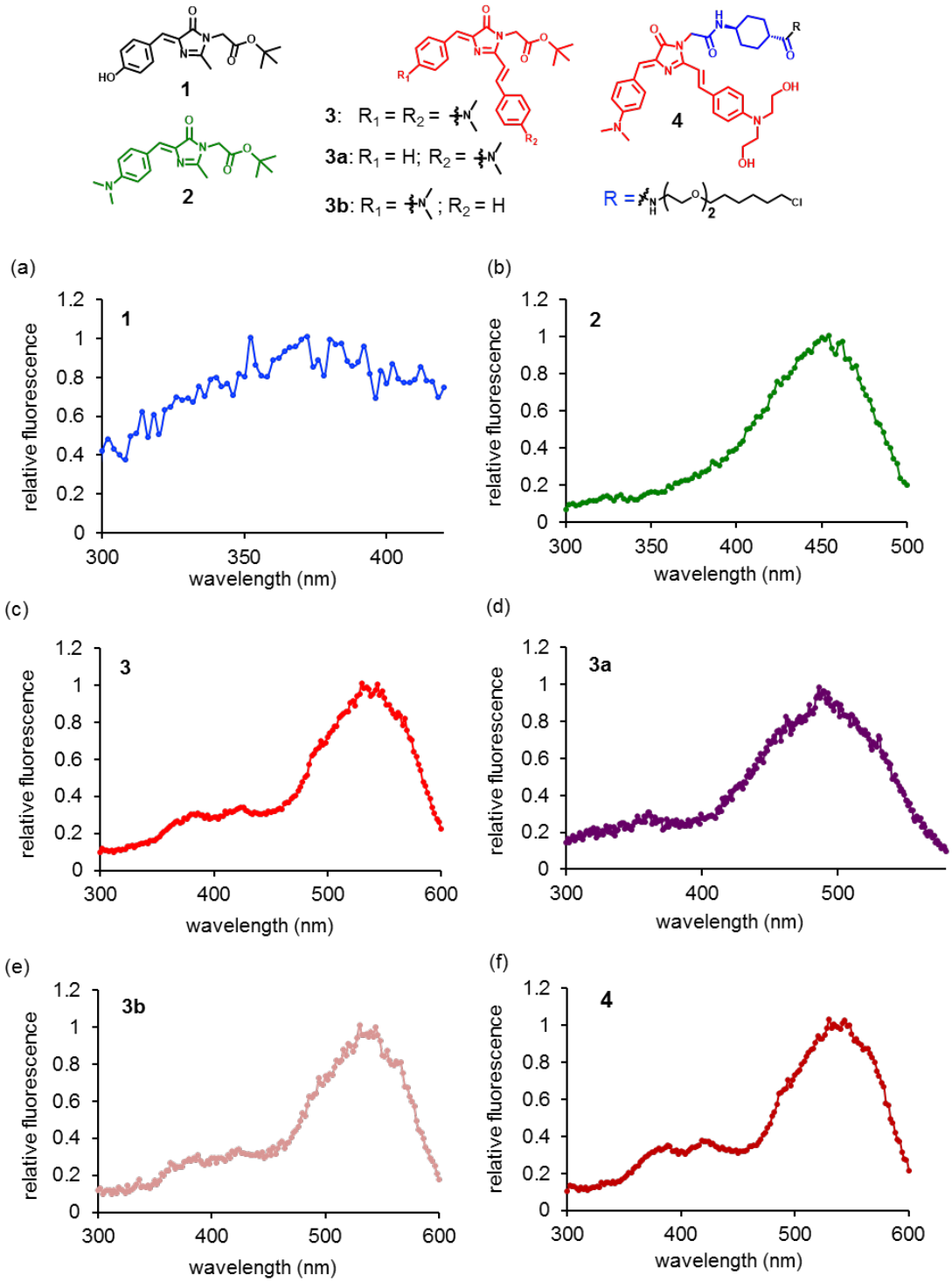

Figure S2: Normalized excitation spectra of FP chromophore analogues in glycerol. FP analogues (20 μM) were prepared in glycerol. Spectra were collected with emission wavelength of 420 nm for **1**, 525 nm for **2**, 620 nm for **3**, **3a**, **3b**, and **4**. All measurements were carried out using a Tecan infinite M1000Pro fluorescence microplate reader.

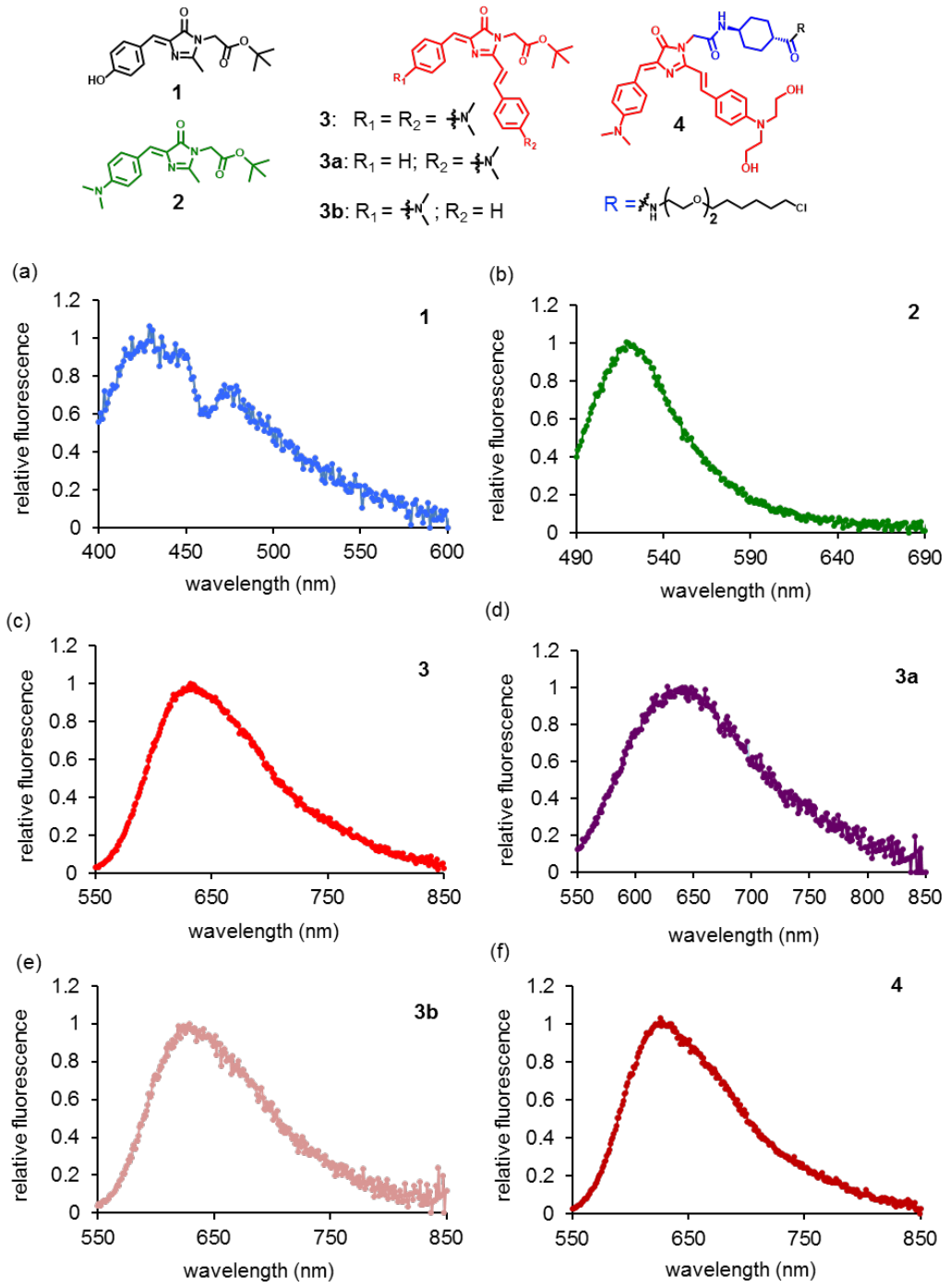

Figure S3: Normalized emission spectra of FP chromophore analogues in glycerol. FP analogues (20 µM) were prepared in glycerol. Spectra were collected with excitation wavelength of 370 nm for **1**, 455 nm for **2**, 530 nm for **3**, **4**, and **3b**, 485 nm for **3a**. All measurements were carried out using a Tecan infinite M1000Pro fluorescence microplate reader.

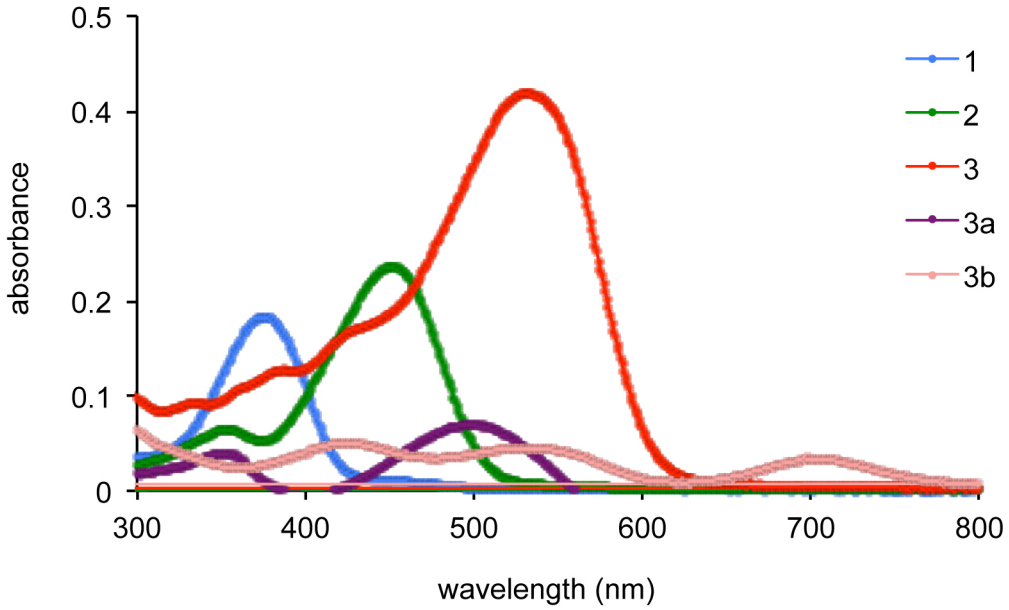

Figure S4: Absorbance spectra of FP chromophore analogues in glycerol. FP analogues (10 μM) were prepared in glycerol. Spectra were collected with 10 mm quartz cuvette. All measurements were carried out using Agilent 300 UV-Vis spectrophotometer.

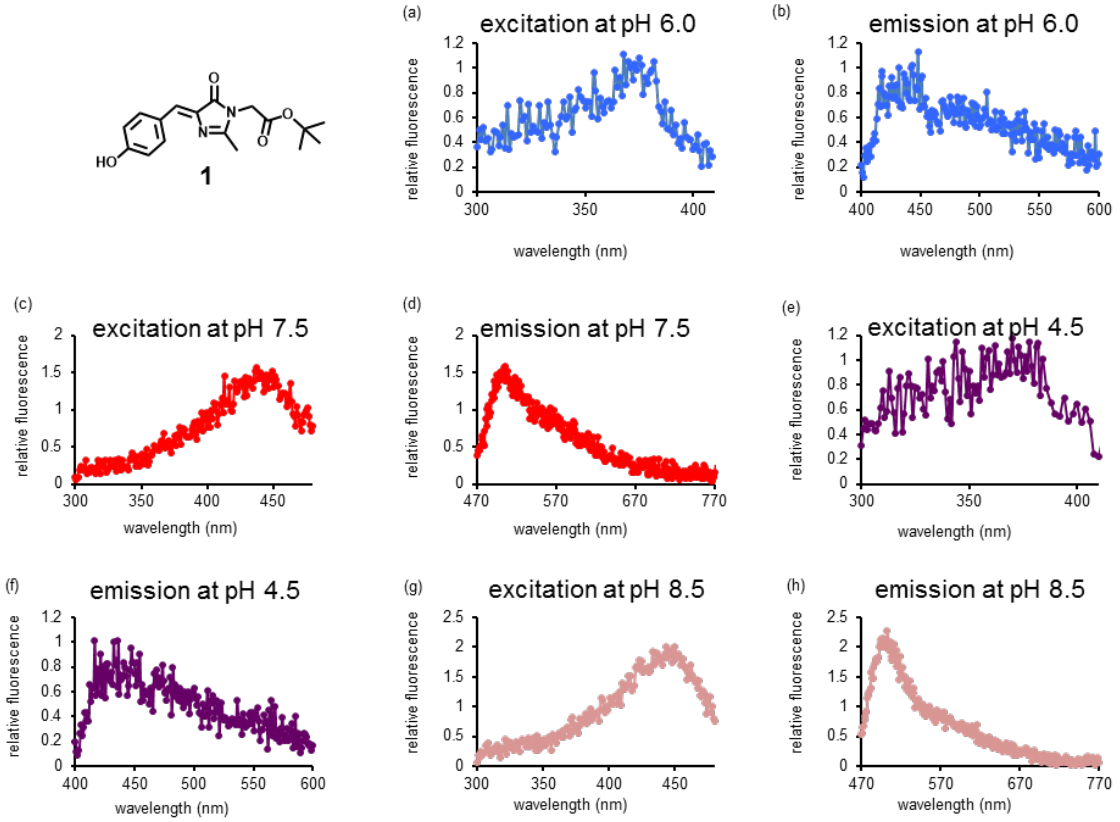

Figure S5: Fluorescence intensity and emission maxima of 1 are pH dependent in glycerol-buffer mixtures. FP analogue **1** (10 μM) was prepared in indicated buffer-glycerol mixtures. (**a**) Excitation spectrum in 90% glycerol/ 10% water. (**b**) Emission spectrum in 90% glycerol/ 10% water. (**c**) Excitation spectrum in 90% glycerol/ 10% PBS. (**d**) Emission spectrum in 90% glycerol/ 10% PBS. (**e**) Excitation spectrum in 90% glycerol/ 10% sodium acetate buffer pH=4.5. (**f**) Emission spectrum in 90% glycerol/ 10% sodium acetate buffer pH=4.5. (**g**) Excitation spectrum in 90% glycerol/ 10% Tris pH=8.5. (**h**) Emission spectrum in 90% glycerol/ 10% Tris pH=8.5. In basic buffer-glycerol mixture, **1** is more fluorescent than in acidic buffer-glycerol mixture. It also exhibited a red shift in in basic solutions. All measurements were carried out using a Tecan infinite M1000Pro fluorescence microplate reader.

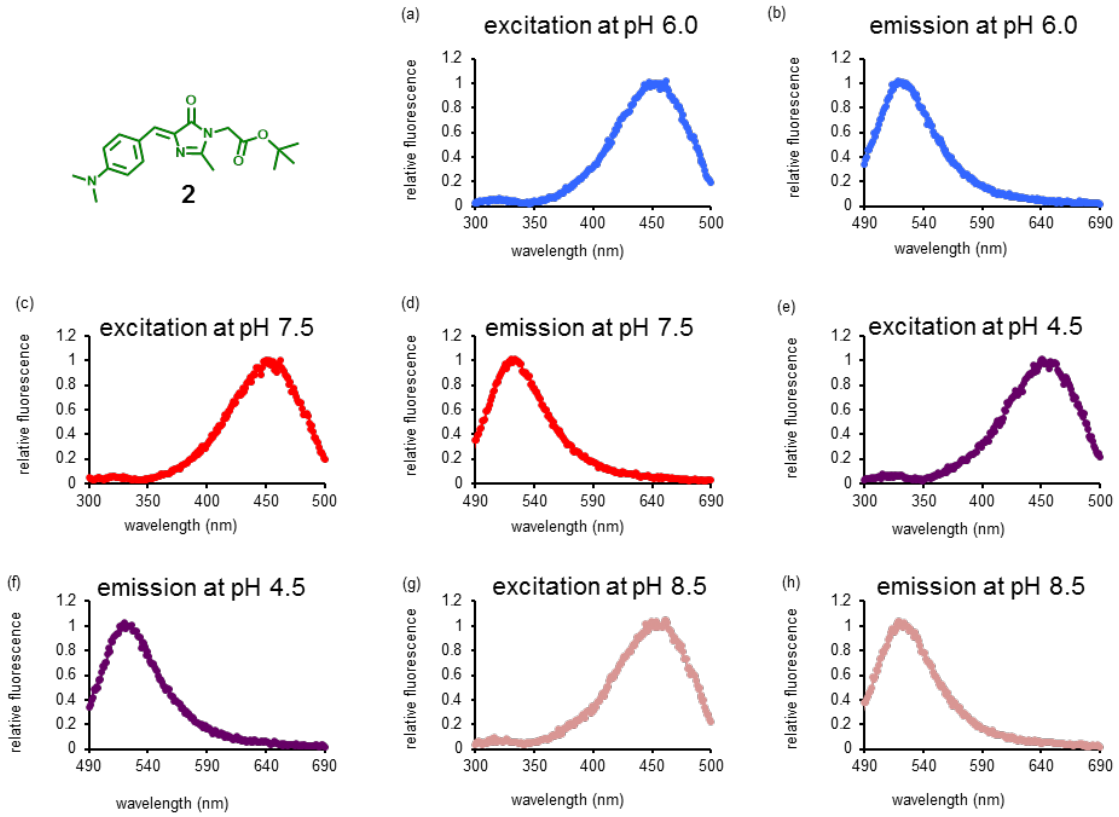

Figure S6: Fluorescence intensity and emission maxima of 2 are insensitive to pH in glycerol-buffer mixtures. FP analogue **2** (10 µM) was prepared in indicated buffer-glycerol mixtures. (**a**) Excitation spectrum in 90% glycerol/ 10% water. (**b**) Emission spectrum in 90% glycerol/ 10% water. (**c**) Excitation spectrum in 90% glycerol/ 10% PBS. (**d**) Emission spectrum in 90% glycerol/ 10% PBS. (**e**) Excitation spectrum in 90% glycerol/ 10% sodium acetate buffer pH=4.5. (**f**) Emission spectrum in 90% glycerol/ 10% sodium acetate buffer pH=4.5. (**g**) Excitation spectrum in 90% glycerol/ 10% Tris pH=8.5. (**h**) Emission spectrum in 90% glycerol/ 10% Tris pH=8.5. All measurements were carried out using a Tecan infinite M1000Pro fluorescence microplate reader.

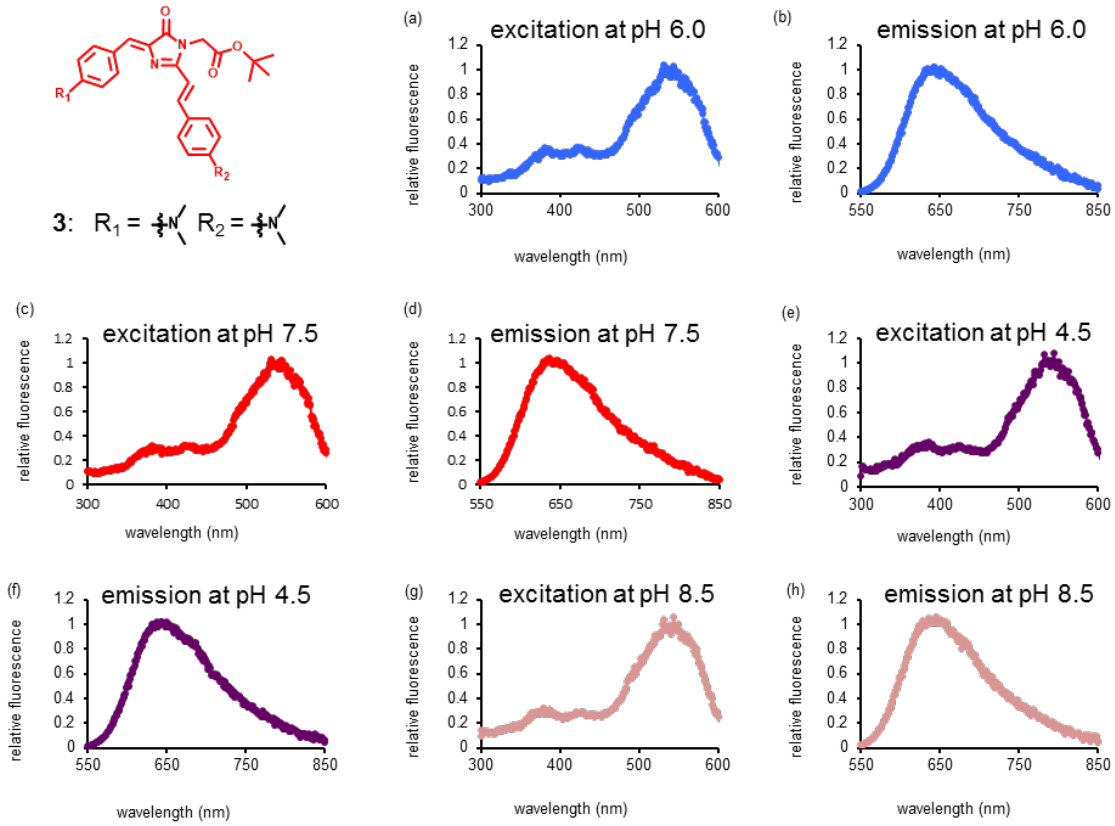

Figure S7: Fluorescence intensity and emission maxima of 3 are insensitive to pH in glycerol-buffer mixtures. FP analogue **3** (10 μM) was prepared in indicated buffer-glycerol mixtures. (**a**) Excitation spectrum in 90% glycerol/ 10% water. (**b**) Emission spectrum in 90% glycerol/ 10% water. (**c**) Excitation spectrum in 90% glycerol/ 10% PBS. (**d**) Emission spectrum in 90% glycerol/ 10% PBS. (**e**) Excitation spectrum in 90% glycerol/ 10% sodium acetate buffer pH=4.5. (**f**) Emission spectrum in 90% glycerol/ 10% sodium acetate buffer pH=4.5. (**g**) Excitation spectrum in 90% glycerol/ 10% Tris pH=8.5. (**h**) Emission spectrum in 90% glycerol/ 10% Tris pH=8.5. All measurements were carried out using a Tecan infinite M1000Pro fluorescence microplate reader.

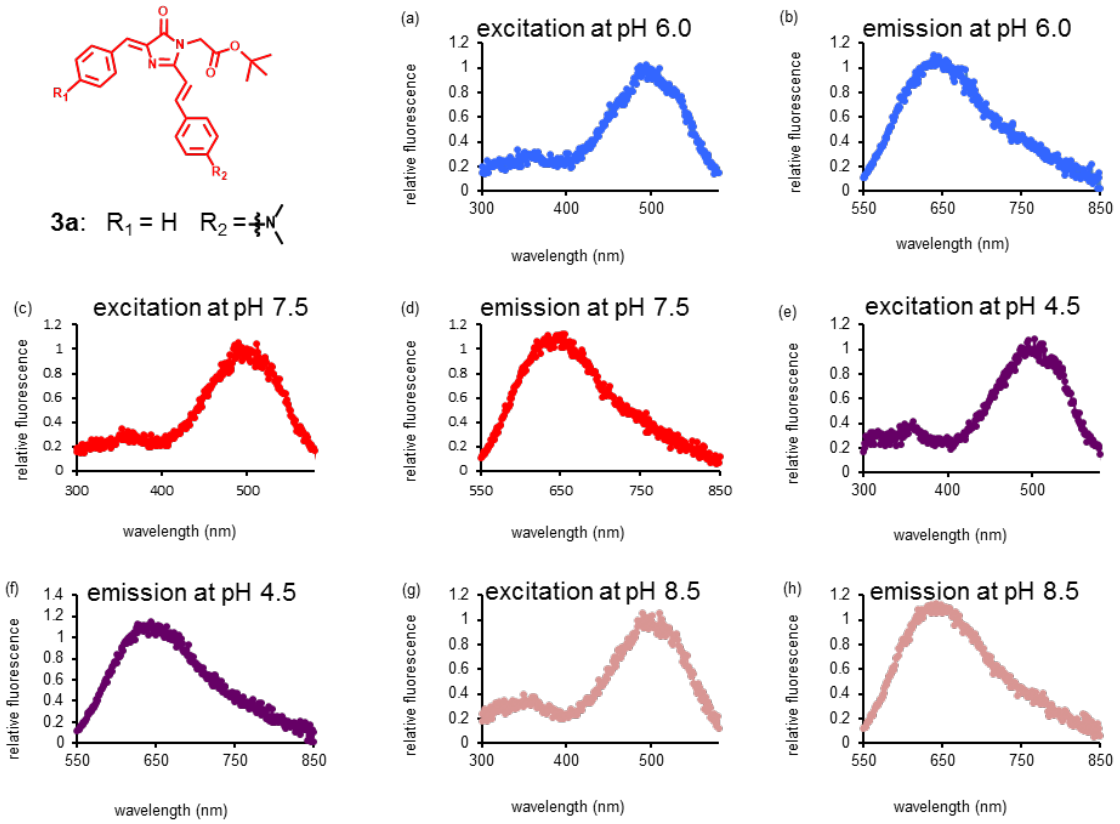

Figure S8: Fluorescence intensity and emission maxima of 3a are insensitive to pH in glycerol-buffer mixtures. FP analogue **3a** (10 µM) was prepared in indicated buffer-glycerol mixtures. (**a**) Excitation spectrum in 90% glycerol/ 10% water. (**b**) Emission spectrum in 90% glycerol/ 10% water. (**c**) Excitation spectrum in 90% glycerol/ 10% PBS. (**d**) Emission spectrum in 90% glycerol/ 10% PBS. (**e**) Excitation spectrum in 90% glycerol/ 10% sodium acetate buffer pH=4.5. (**f**) Emission spectrum in 90% glycerol/ 10% sodium acetate buffer pH=4.5. (**g**) Excitation spectrum in 90% glycerol/ 10% Tris pH=8.5. (**h**) Emission spectrum in 90% glycerol/ 10% Tris pH=8.5. All measurements were carried out using a Tecan infinite M1000Pro fluorescence microplate reader.

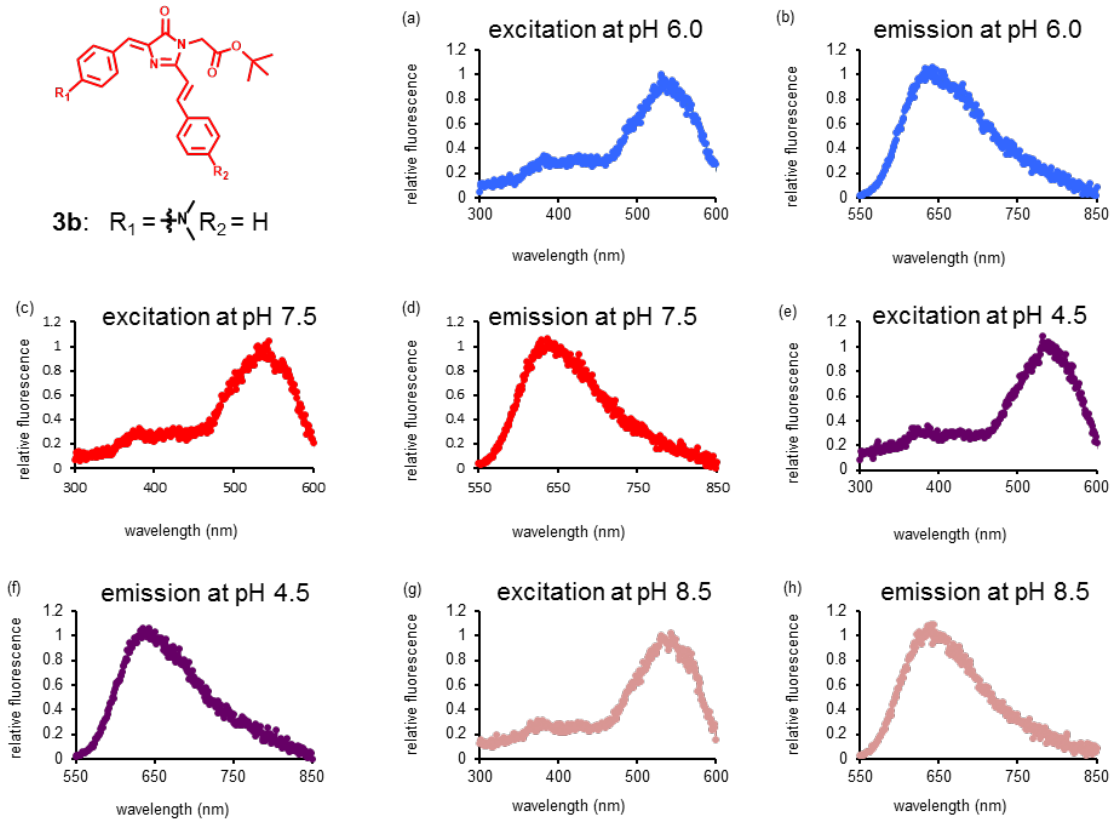

Figure S9: Fluorescence intensity and emission maxima of 3b are insensitive to pH in glycerol-buffer mixtures. FP analogue **3b** (10 µM) was prepared in indicated buffer-glycerol mixtures. (**a**) Excitation spectrum in 90% glycerol/ 10% water. (**b**) Emission spectrum in 90% glycerol/ 10% water. (**c**) Excitation spectrum in 90% glycerol/ 10% PBS. (**d**) Emission spectrum in 90% glycerol/ 10% PBS. (**e**) Excitation spectrum in 90% glycerol/ 10% sodium acetate buffer pH=4.5. (**f**) Emission spectrum in 90% glycerol/ 10% sodium acetate buffer pH=4.5. (**g**) Excitation spectrum in 90% glycerol/ 10% Tris pH=8.5. (**h**) Emission spectrum in 90% glycerol/ 10% Tris pH=8.5. All measurements were carried out using a Tecan infinite M1000Pro fluorescence microplate reader.

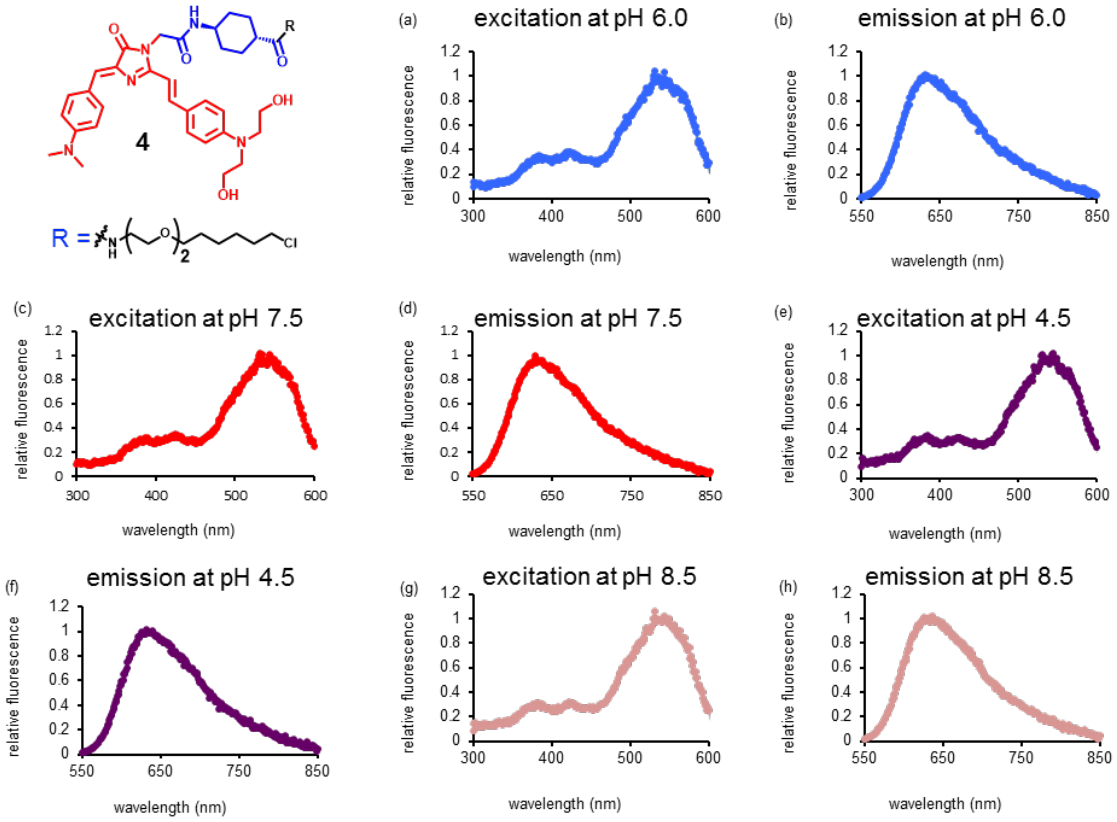

Figure S10: Fluorescence intensity and emission maxima of 4 are insensitive to pH in glycerol-buffer mixtures. FP analogue **4** (10 μM) was prepared in indicated buffer-glycerol mixtures. (**a**) Excitation spectrum in 90% glycerol/ 10% water. (**b**) Emission spectrum in 90% glycerol/ 10% water. (**c**) Excitation spectrum in 90% glycerol/ 10% PBS. (**d**) Emission spectrum in 90% glycerol/ 10% PBS. (**e**) Excitation spectrum in 90% glycerol/ 10% sodium acetate buffer pH=4.5. (**f**) Emission spectrum in 90% glycerol/ 10% sodium acetate buffer pH=4.5. (**g**) Excitation spectrum in 90% glycerol/ 10% Tris pH=8.5. (**h**) Emission spectrum in 90% glycerol/ 10% Tris pH=8.5. All measurements were carried out using a Tecan infinite M1000Pro fluorescence microplate reader.

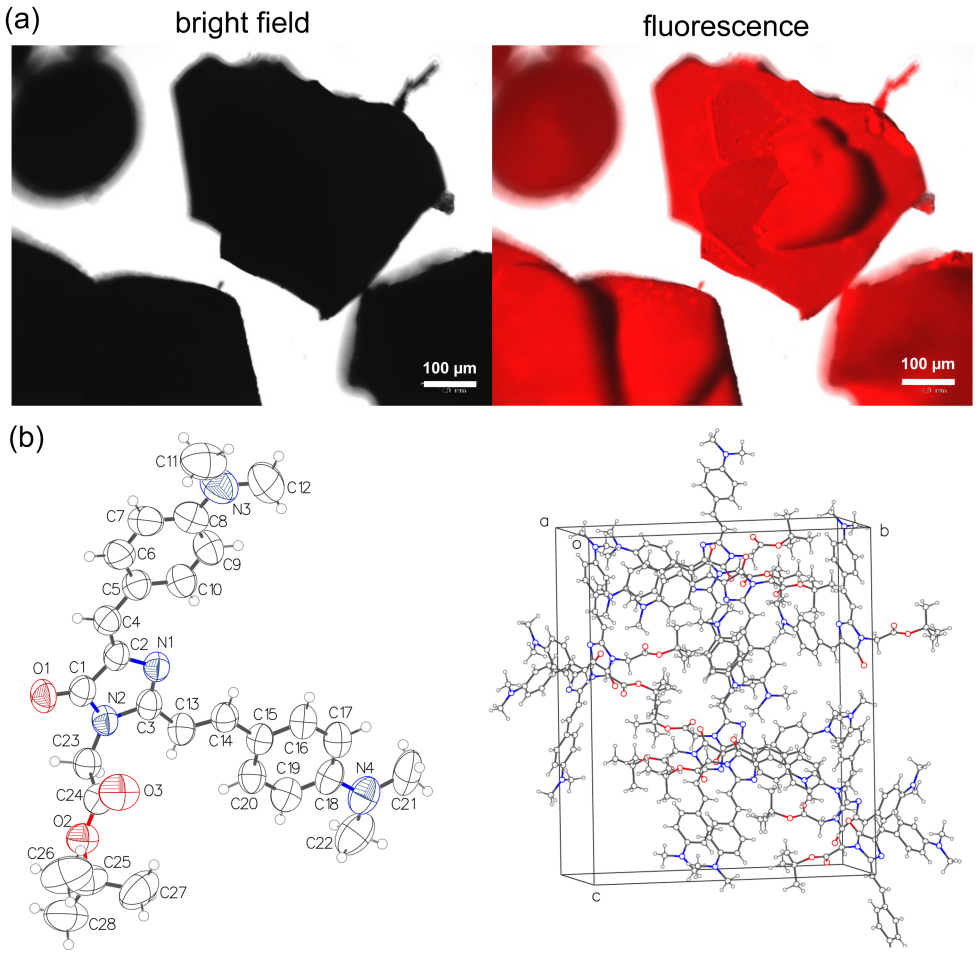

Figure S11.The crystal structure of 3. (**a**) The crystal of **3** is fluorescent. The crystals were looped out and transferred to a 35 mm glass bottom dish. Images were taken using an inverted Biorad ZOE fluorescent cell imager. This data suggests that **3** in the crystal structure should adopt conformation that is fluorescent. Reason of the dark image in the bright field is because light of an inverted microscope could not pass through the thick crystal. (**b**) Crystal structure and packing diagram of 3, with thermal ellipsoids drawn at 50% probability level.

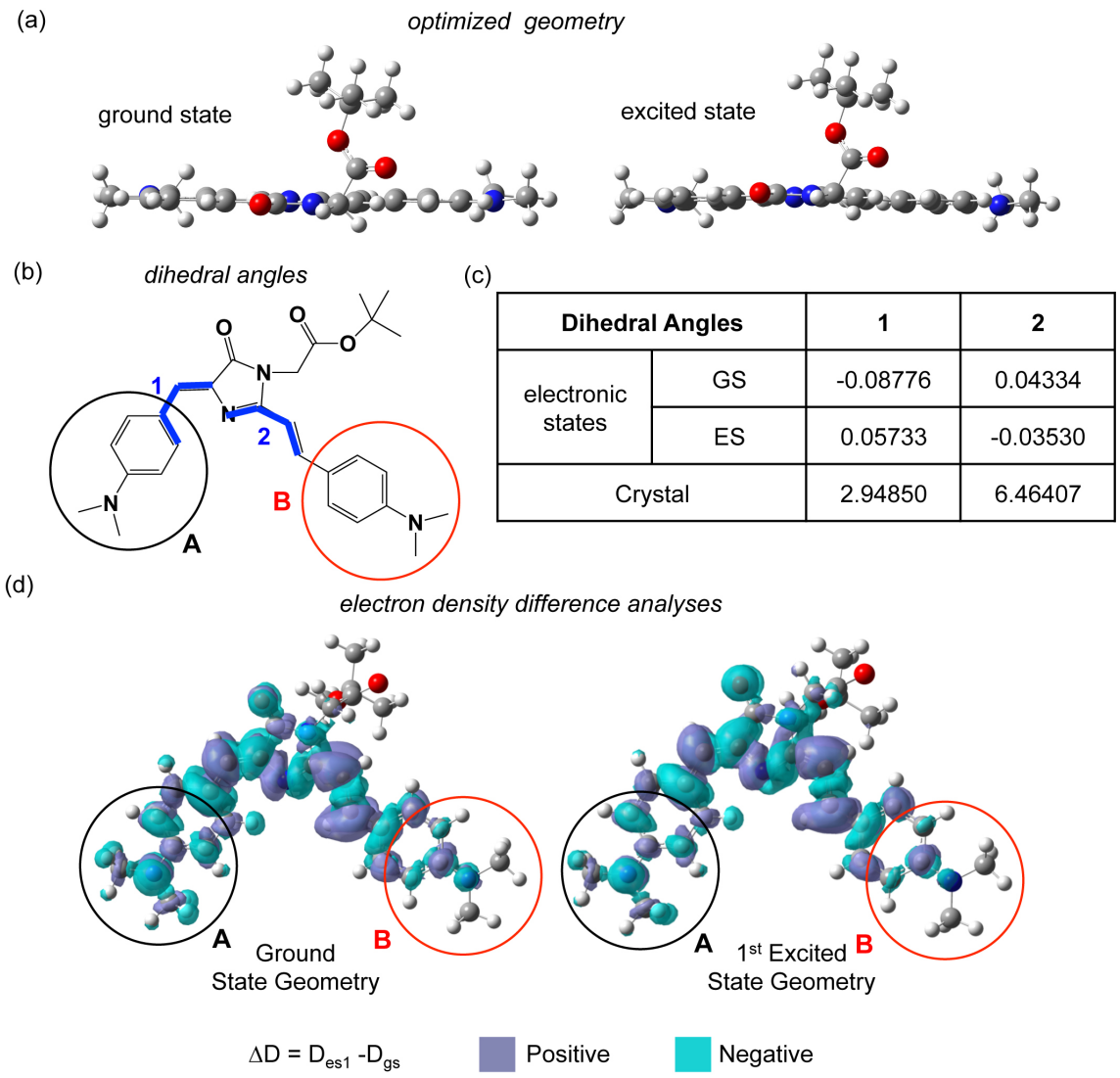

Dihedral Angles		1	2
electronic states	GS	-0.08776	0.04334
	ES	0.05733	-0.03530
Crystal		2.94850	6.46407

Figure S12. Computational analyses of 3 validate its planar S1 excited state structure as the fluorescent state and identify the charge separation at S1 excited state. (**a**) The optimized geometries of **3** in ground state and excited state. (**b-c**) A dihedral angle analysis confirmed planar structures of **3** in both ground state (GS) and excited state (ES). (**d**) Charge density difference isosurfaces (isovalue = 0.0004) at the minimum energy conical intersection between ground state and S1 excited state. Positive isosurfaces are blue and indicate electron withdraw. Negative isosurfaces are cyan and indicate electron donation. This data suggests that group A is the primary electron donor that contributes to charge separation at S1 excited state.

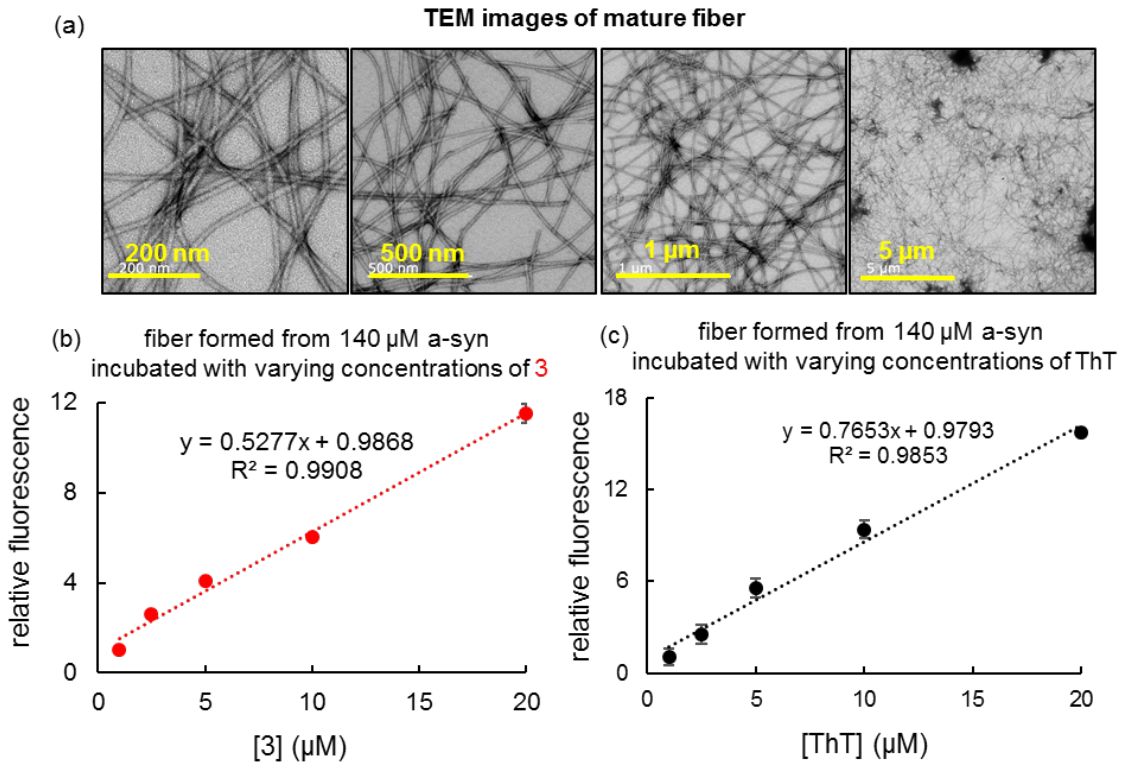

Figure S13. Fluorogenic detection of mature α-synuclein fibers using 3 or ThT. (**a**) Electron micrographs of α-synuclein fibrils formed at 72 h. Images were taken at different resolutions. Scale bars: 200 nm, 500 nm, 1 µm, and 5 µm. (**b-c**) Fluorescence intensity of **3** (**b**) or ThT (**c**) is proportional to probe concentrations present in α-synuclein fibrils. Aggregation of α-synuclein (140 µM) was performed in presence of probe **3** or ThT of increasing but sub-stoichiometric concentrations (1 to 20 µM). We observed that fluorescence intensity is proportional to the amount of probe **3** present in the assay. The linear correlation between fluorescence intensity and probe **3** concentration indicates that fluorescence of **3** originated from α-synuclein fibers. As a control experiment, similar observations were made using ThT (Thioflavin T), a standard amyloid probe. Aggregation of α-synuclein was carried out using method described in the Supporting Information. Parameters for fluorescence measurement: **3** (E_x = 530 nm/E_m = 600 nm) and ThT (E_x = 440 nm/E_m = 480 nm). Error bars: standard error (n=3).

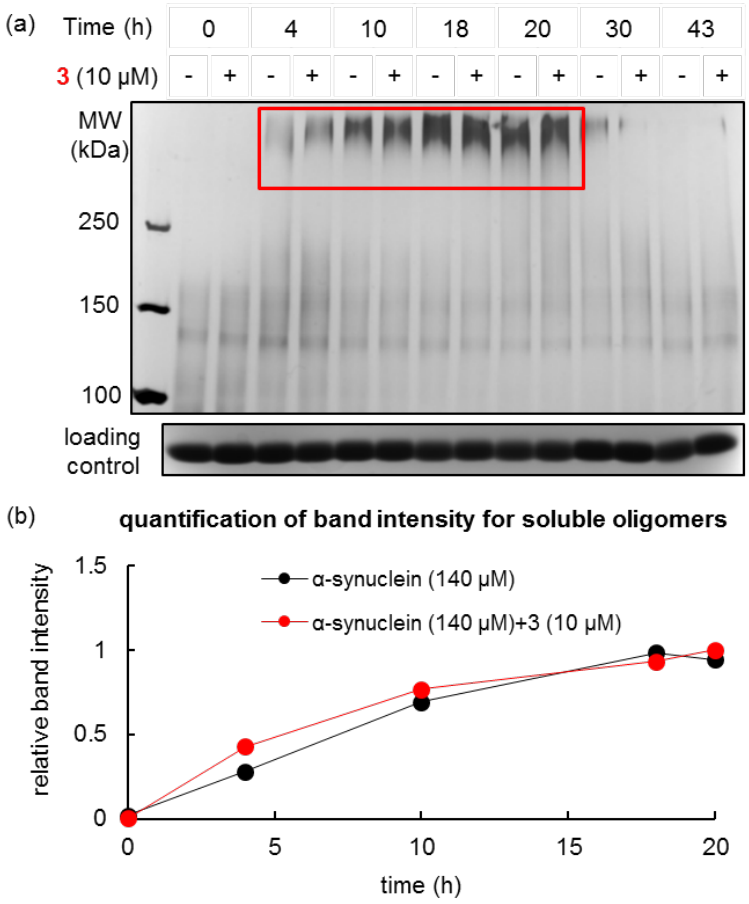

Figure S14. Chemical crosslinking experiment reveals formation of soluble oligomers during α-synuclein aggregation. (**a**) SDS-PAGE (visualized by silver stain) analysis of chemically crosslinked soluble oligomers of α-synuclein. Oligomers started to form at 4 h and accumulated up to 20 h during the lag phase. Disappearance of soluble oligomers occurred during fiber growth and maturation after 20 h. (**b**) No significant difference in the amount of soluble oligomers was detected with or without probe **3** during aggregation. Aggregation of α-synuclein (140 μM) was performed in low binding Eppendorf tubes with agitation (1350 rpm) at 37 °C for 43 h in absence or presence of probe 3 (10 μM). Assay buffer is 20 mM HEPES, 100 mM NaCl at pH 7.5. Samples were taken at indicated time points and chemically crosslinked with DSS (disuccinimidyl suberate, 1.5 mM) for 30 min at room temperature according to manufacturer's instructions. 1 M Tris buffer was added to the final concentration of 20 mM to quench the crosslinking reaction for 15 min and immediately boiled with SDS loading buffer. Samples were resolved using 5% Tris-Glycine SDS-Page gel. To visualize the crosslinked species of higher molecular weights, the gel was stained using Pierce Silver Stain Kit (Prod # 24612). Non-crosslinked samples were resolved using 15% Tris-Glycine SDS-Page gel for loading control purpose and stained using standard coomassie blue.

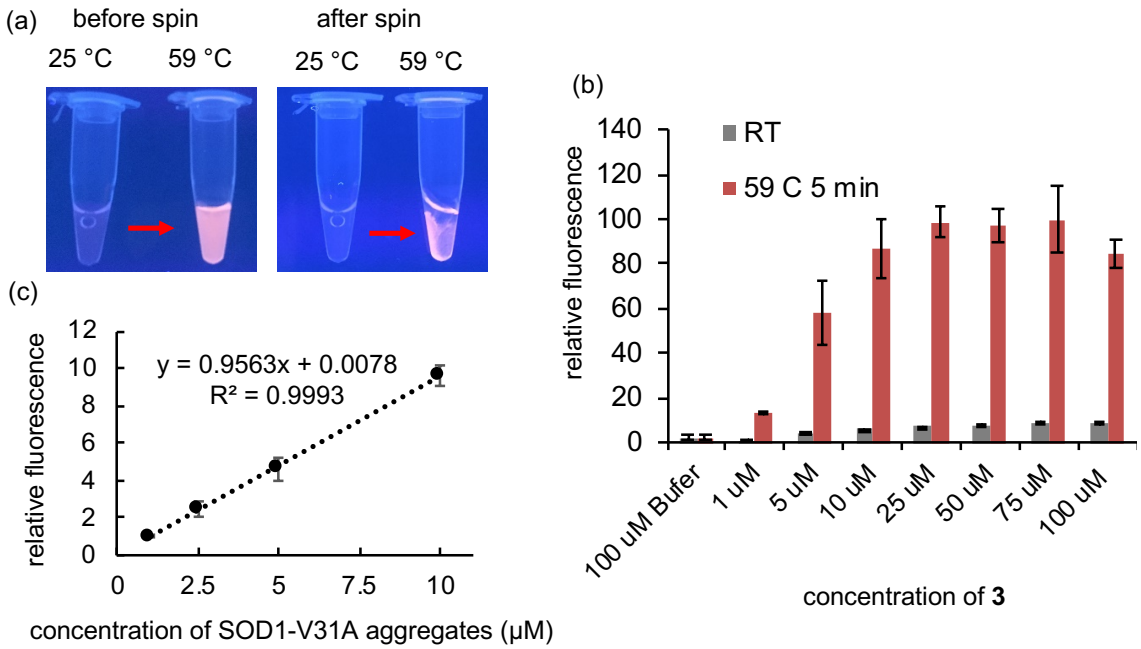

Figure S15. Fluorogenic detection of SOD1(V31A) aggregates using 3. (**a**) SOD1(V31A) aggregation (42 µM) was induced at 59 ºC for 30 min in buffer (50 mM Tris-HCl, pH 7.5, 100 mM NaCl, 83 mM EDTA), in the presence of **3** (21 µM). Reaction mixture was illuminated by UV trans-illuminator before and after centrifugation at 21,000 g for 10 min at 4 ºC. (**b**) Fluorescence intensity of SOD1(V31A) aggregates (42 µM) in the presence of varying concentrations of **3**. 100 µM of 3 in buffer was used as a control. Parameters for fluorescence measurement: **3** (E_x = 530 nm/E_m = 600 nm). Error bars: standard error (n=3). (**c**) Fluorescence intensity of SOD1(V31A) aggregates (1, 2.5, 5, 10 µM) in the presence of 20 µM of **3**. Parameters for fluorescence measurement: **3** (E_x = 530 nm/E_m = 600 nm). Error bars: standard error (n=3).

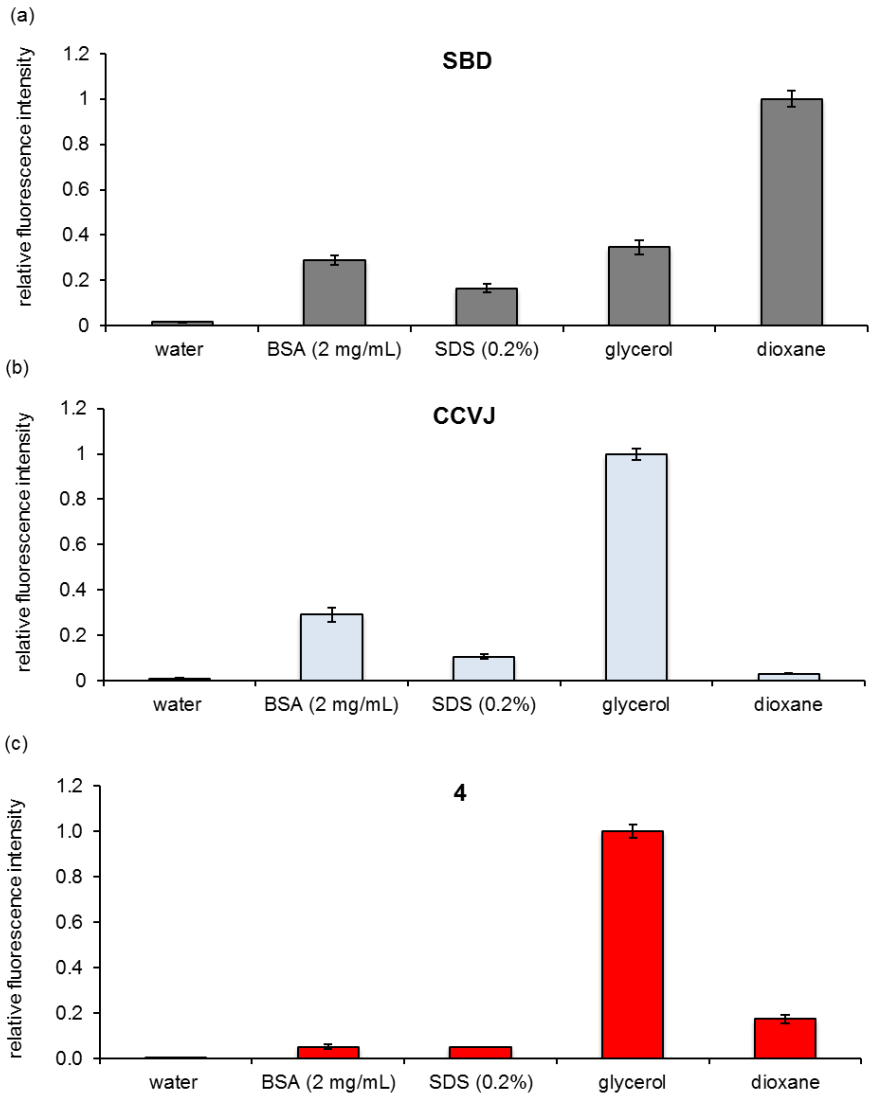

Figure S16: Fluorescence response of SBD, CCVJ, and 4 to BSA and SDS. 20 μM of fluorophores were incubated in H_2O, glycerol, dioxane, BSA (2 mg/mL), or SDS (0.2 %). Intensities were normalized against the value in either 100% glycerol as 1 for CCVJ and **4**, or dioxane as 1 for SBD. Parameters for fluorescence measurement: SBD (E_x = 450 nm/E_m = 545 nm), CCVJ (E_x = 450 nm/E_m = 500 nm), **4** (E_x = 530 nm/E_m = 630 nm). Error bars: standard error (n=3).

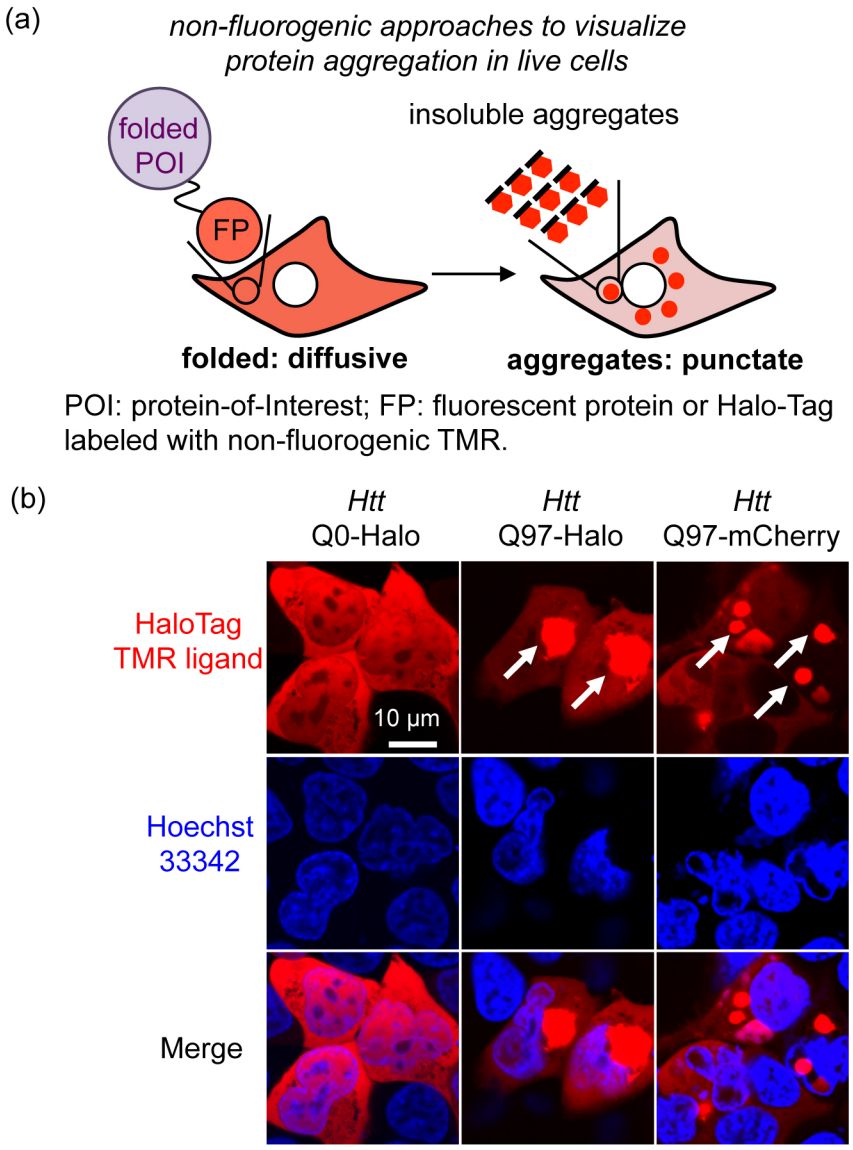

Figure S17: Confocal fluorescent images of *Htt* Q0-Halo, *Htt* Q97-Halo and *Htt* Q97-mCherry in HEK293T cells. (**a**) Schematic diagram for classic non-fluorogenic imaging approaches to visualize protein aggregates in live cells, via identification of fluorescent punctate structures due to the slower diffusion rate of insoluble aggregates than soluble proteins. (**b**) The *Htt* Q0-Halo, *Htt* Q97-Halo and *Htt* Q97-mCherry proteins were transiently transfected and expressed HEK293T cells for 24 h. 1 μM TMR Halo-Tag ligand was added during protein expression to covalently label the *Htt* Q0-Halo and *Htt* Q97-Halo proteins. In cells expressing *Htt* Q97 proteins, obvious punctate structures (white arrows) were found in the background of diffuse fluorescence. Whereas, only diffuse fluorescence was observed in cells expressing the *Htt* Q0 protein (upper panel). Red: HaloTag-TMR or mCherry. Blue: nucleus stained by Hoechst 33342. Scale bar: 10 μm.

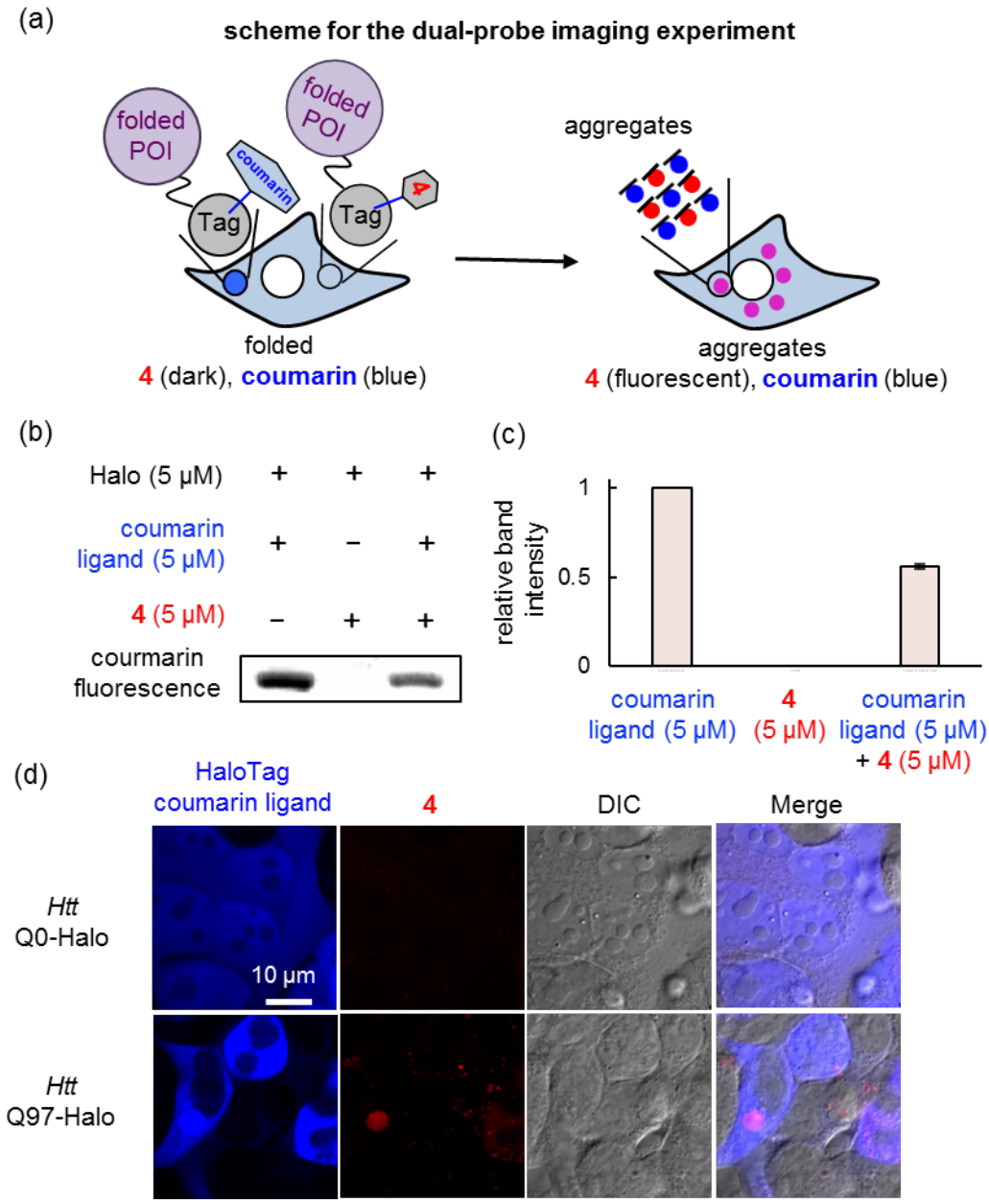

Figure S18: Fluorogenic detection of *Htt* Q97-Halo aggregation in HEK293T cells. (**a**) The dual-probe live cell imaging experimental scheme. Halo-tag fusion proteins were co-labeled in the presence of both the non-fluorogenic coumarin ligand (1 μM) and **4** (1 μM). The newly synthesized *Htt*-Halo proteins were co-labeled with either the coumarin ligand or **4**. The coumarin ligand is fluorescent both before and after aggregation of *Htt*-Halo. By contrast, signal of **4** exclusively arises from *Htt*-Halo aggregates. (**b**) & (**c**) Purified Halo protein (5 μM) can be equally labeled using coumarin ligand (5 μM) and probe **4** (5 μM). (**d**) The *Htt* Q0-Halo and *Htt* Q97-Halo proteins were transiently transfected and expressed in HEK293T cells for 24 h, in the presence of 1 μM coumarin Halo-Tag ligand and 1 μM of **4**. In cells expressing *Htt* Q97-Halo proteins, punctate structures in the coumarin channel

coincided with the turn-on fluorescence of **4**. Whereas, only diffuse coumarin fluorescence was observed in cells expressing the *Htt* Q0-Halo protein and no turn-on fluorescence of **4** was found. Blue: coumarin Halo-Tag ligand. Red: fluorescence of **4**. Scale bar: 10 μm.

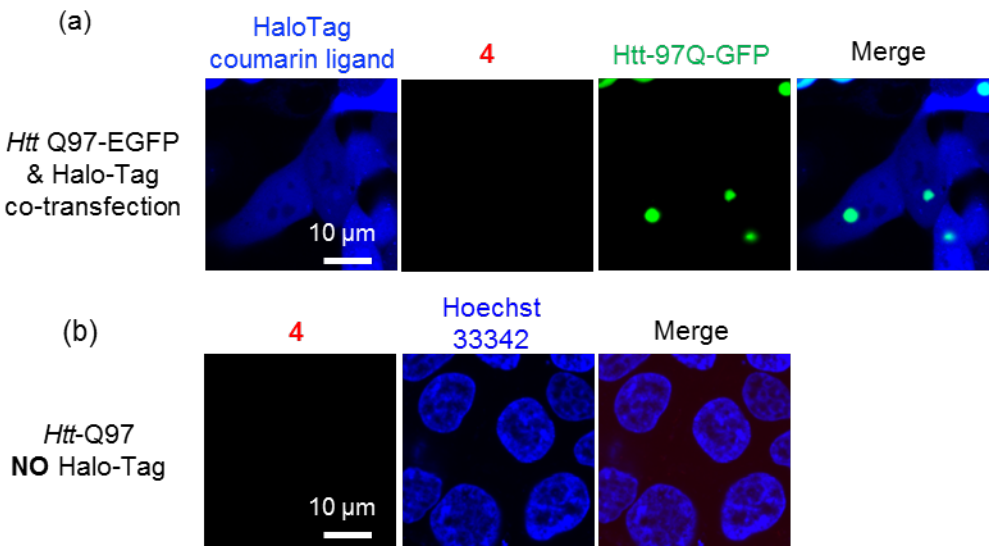

Figure S19. Fluorescence turn-on signal of 4 induced by aggregation of protein-of-interest (POI) requires covalent and genetic fusion of HaloTag for intramolecular interaction of probe 4 with the aggregated POI. (**a**) No fluorescence was observed from the Halo•4 conjugate in cells co-transfected with *Htt*-Q97-EGFP and Halo-Tag. Expression of Halo-Tag was evidenced by fluorescence of the Halo•coumarin conjugate in the blue channel. Expression of *Htt* Q97-EGFP was evidenced by the GFP signal in the green channel. Aggregation of *Htt* Q97-EGFP was shown by puncta formation. HEK293T cells were seeded in 35 mm PDK-coated imaging chamber and reached 50%-60% confluency. Cells were transiently co-transfected with *Htt* Q97-EGFP and Halo, and labeled with 1 µM **4** and 1 µM coumarin Halo-Tag ligand to simultaneously form covalent conjugate with the Halo-Tag domain. After 48 h expression, medium was replaced with fresh DMEM to diffuse out unbound ligands prior to confocal imaging. Scale bar: 10 µm. (**b**) No turn-on fluorescence of **4** was found in cells transfected with *Htt*-Q97. The *Htt*-Q97 protein, without a Halo-Tag, was transiently transfected and expressed in HEK293T cells for 24 h, in the presence of 1 µM of **4**. No turn-on fluorescence of **4** was found.

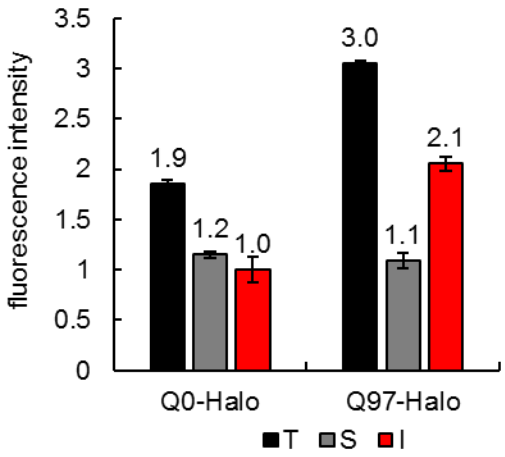

Figure S20. Quantification of fluorescence intensity in fractionated cellular lysate expressing Q97-Halo and Q0-Halo protein. Fluorescent intensity of cell lysates from samples as represented in **Figure 4d**.

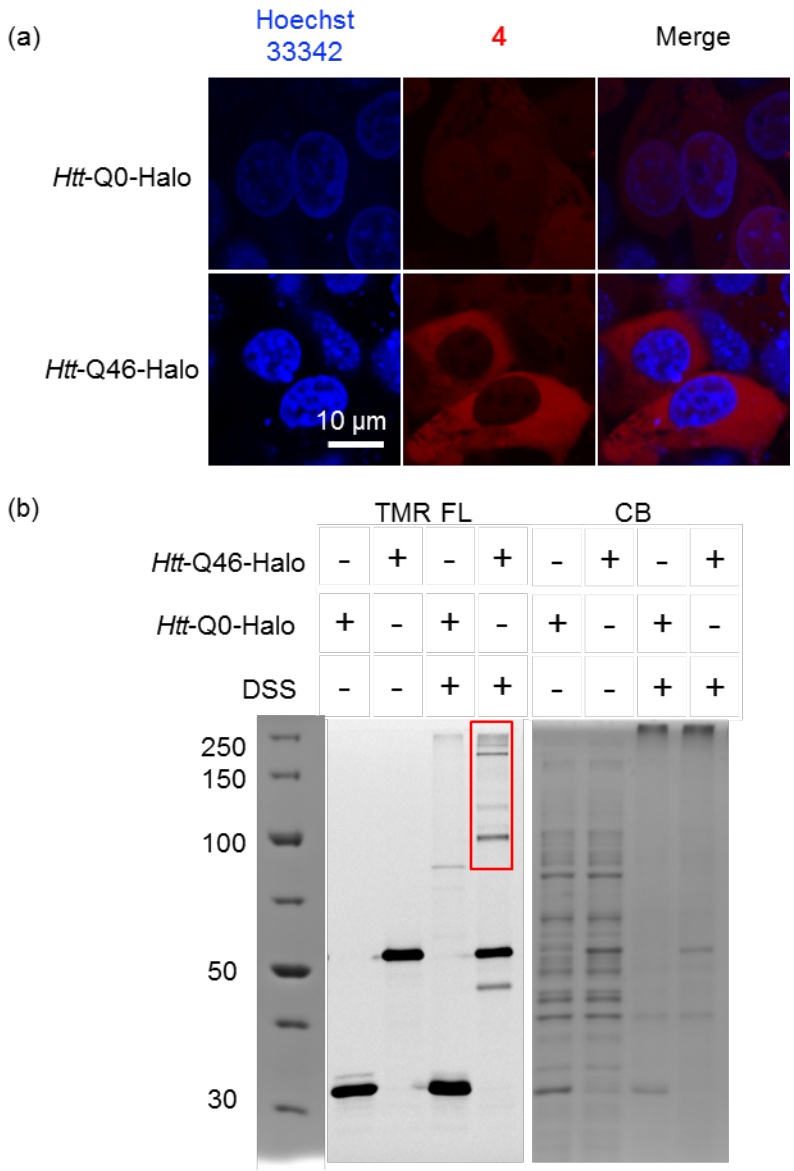

Figure S21. *Htt*-Q46 forms soluble oligomers. (**a**) Confocal images of *Htt*-Q0-Halo and *Htt*-Q46-Halo. Stronger diffuse red fluorescence was observed using fluorogenic probe **4** in HEK293T cells transiently expressing *Htt*-46Q-Halo for 48 h, indicating formation of soluble oligomers. (**b**) Chemical crosslinking experiment showed formation of *Htt*-Q46 soluble oligomers in HEK293T cells. Left: 10% SDS-PAGE gel visualized by TMR fluorescence. Right: Coomassie blued stained gel to show the amount of total protein loaded on the gel. HEK293T cells transiently expressing *Htt*-Q46-Halo for 48 h were incubated in presence of 1 μM TMR HaloTag ligand to form the fluorescent conjugate for visualization purpose on SDS-PAGE gel. Freshly prepared DSS (disuccinimidyl suberate, Thermo Scientific™) in DMSO was added into samples to a final concentration of 5 mM DSS and incubated at room temperature for 30 min. Crosslinking reaction were then quenched with addition of 1 M Tris buffer to a final concentration of 100 mM Tris to neutralize the reactivity of NHS ester. Cells were lysed by sonication for 1 min (20%

amplitude, 1 s on, 2 s pulse). Samples were centrifuged for 30 min at 21,000 g at 4 ºC. Soluble fraction was sampled and boiled with SDS loading buffer before resolved by SDS-Page gel. Cell numbers were normalized to the same and lysate concentration was further normalized by Bradford assay before loading on the gel. *Htt*-Q46-Halo showed higher molecular weight species (highlighted in red box) than *Htt*-Q0-Halo, indicating formation of soluble oligomers.

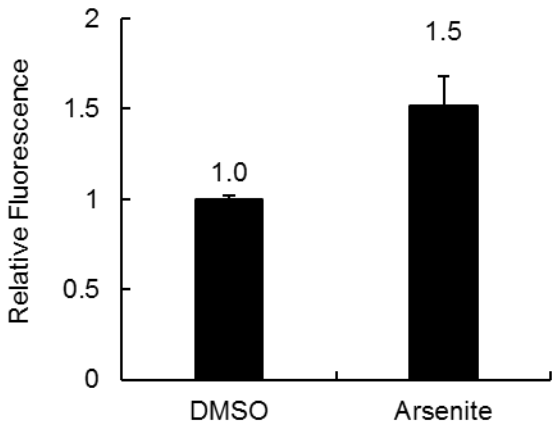

Figure S22. Quantification of fluorescence intensity in cellular lysate expressing SOD1(V31A)-Halo before and after stress. Fluorescent intensity of cell lysates from samples as represented in **Figure 5a**. Fluorescence intensity was taken by Tecan fluorescence plate reader and normalized to the same cell number. Error bars: standard error (n=3).

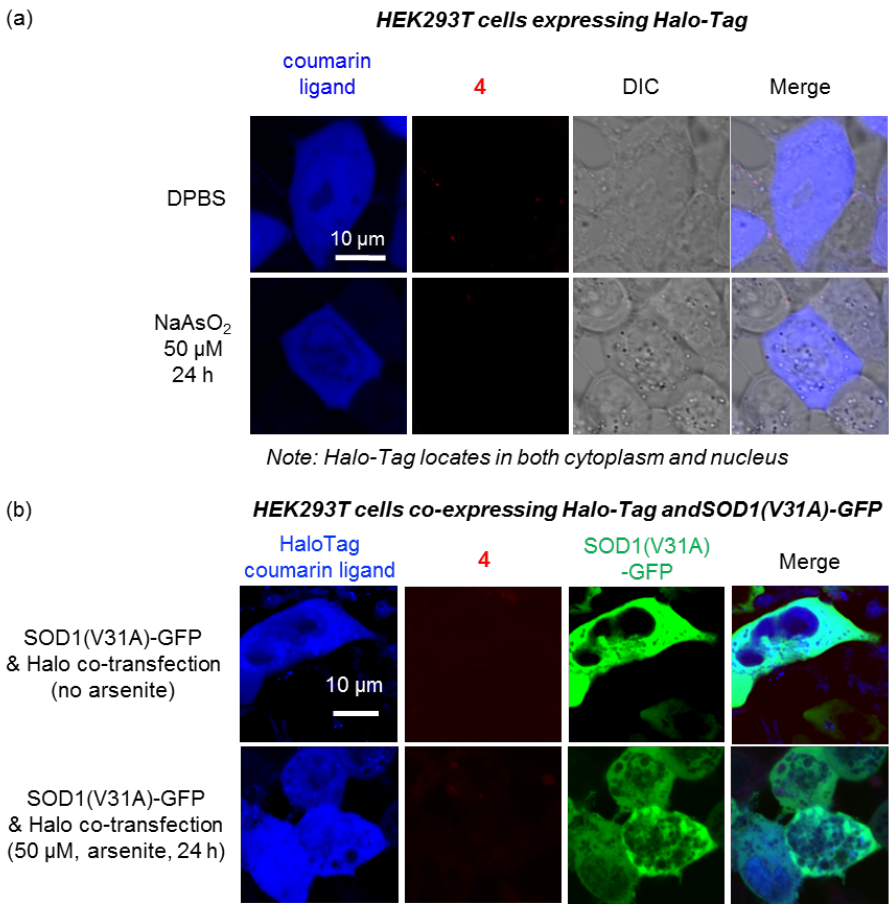

Figure S23. Fluorescence turn-on signal of 4 induced by aggregation of protein-of-interest (POI) requires covalent and genetic fusion of HaloTag for intramolecular interaction of probe 4 with the aggregated POI. (**a**) No turn-on fluorescence of **4** was found before and after stress, indicating that Halo-Tag does not aggregate and turn on the fluorescence of **4**. The Halo-Tag protein, without SOD1(V31A), was transiently transfected and expressed in HEK293T cells for 24 h, in the presence of 1 μM of **4**. (**b**) No turn-on fluorescence was observed in both stressed (50 μM $NaAsO_2$, 24 h) or non-stressed cells co-transfected with SOD1(V31A)-GFP and Halo-Tag. Expression of Halo-Tag was evidenced by fluorescence of the Halo•coumarin conjugate. Expression of of SOD1(V31A)-EGFP was evidenced by the GFP fluorescence. HEK293T cells were seeded in 35 mm PDK-coated imaging chamber and reached 50%-60% confluency. Cells were transiently co-transfected with SOD1(V31A)-GFP and Halo-Tag. Cells were treated and labeled, during a 24-h transfection, with 1 μM **4** and 1 μM coumarin Halo-Tag ligand to simultaneously form covalent conjugate with the Halo-Tag domain. After 24 h expression, medium was replaced with fresh DMEM to diffuse out unbound ligands. After 30 min, media was replaced by fresh DMEM medium containing DMSO vehicle or $NaAsO_2$ (50 μM). Cells were incubated for 24 h at 37 ºC in a CO_2 incubator prior to confocal imaging. Scale bar: 10 μm.

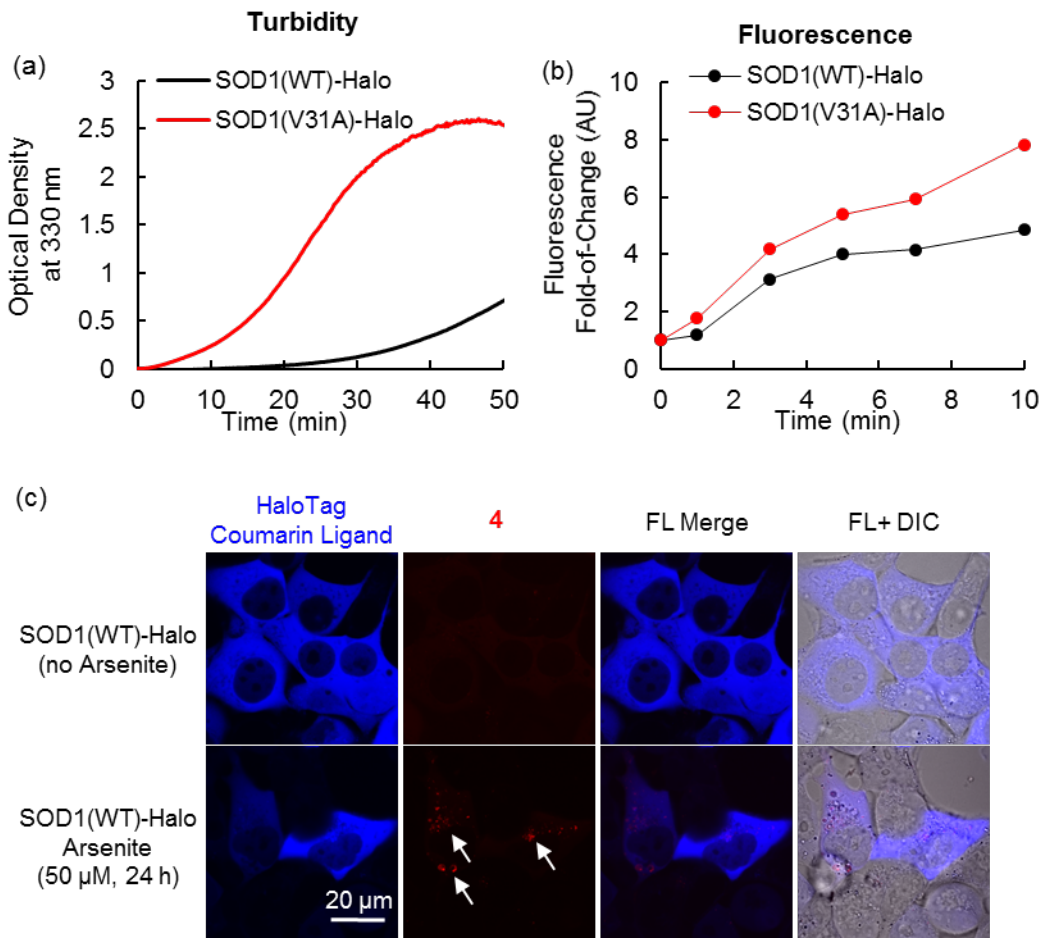

Figure S24. Wild type SOD1 is less aggregation prone than V31A mutant both in buffer and in live cells. (**a**) SOD1(WT)-Halo exhibited slower kinetics than SOD1(V31A)-Halo in heat-induced aggregation as measured by turbidity assay. Purified SOD1(WT)-Halo or SOD1(V31A)-Halo (42 μM) was conjugated with **4** (21 μM) and incubated at 54.5 °C. Turbidity was recorded using Agilent 300 UV-Vis spectrophotometer. Buffer condition: 50 mM Tris-HCl, pH 7.5, 100 mM NaCl, 83 mM EDTA. (**b**) Fluorescence increases from the misfolding and aggregation of SOD1(WT)-Halo is less than that of SOD1(V31A)-Halo. Fluorescence was recorded using Agilent Carey Eclipse fluorescence spectrophotometer with temperature control. Experiments were carried out at 54.5 °C. Parameters for fluorescence measurement: **4** (Ex = 530 nm/Em = 600 nm). (**c**) Aggregation of WT SOD1 in HEK293T cells is less severe than V31A SOD1 mutant upon arsenite induced oxidative stress shown by fluorogenic probe **4**. Upper panel: no red fluorescence was observed using **4** in the unstressed sample. Lower panel: small fluorescent puncta were observed using **4** in the stressed sample (highlighted by white arrows). Different from V31A mutant (**Figure 5a**), no diffuse fluorescence was observed and less puncta formed for WT SOD1 upon stress. Another difference we observed for SOD1(WT)-Halo is that less translocation into nucleus occurred upon stress. Experimental procedures are the same as experiments in **Figure 5a**.

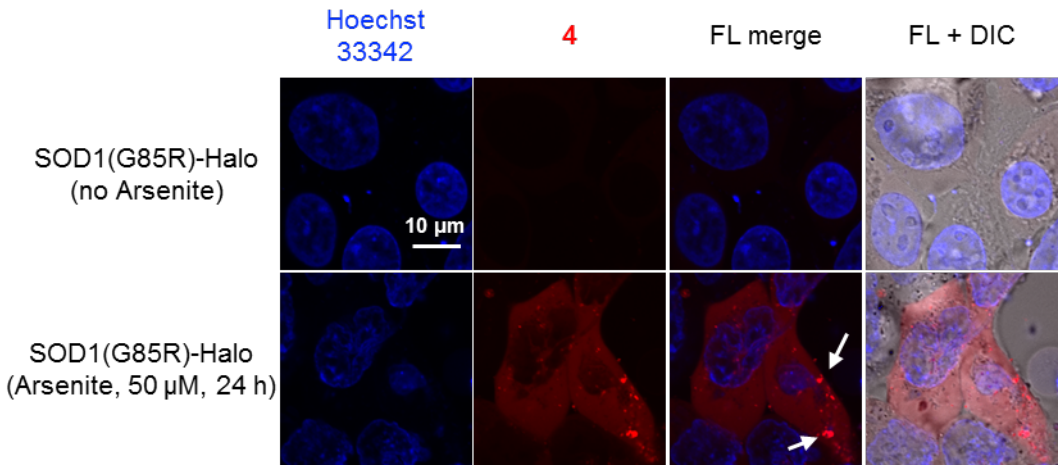

Figure S25. SOD1(G85R)-Halo exhibited both diffuse and punctate fluorescence upon arsenite induced stress. SOD1(G85R)-Halo was transiently expressed for 24 h and labeled with 1 μM **4** during expression. After excessive **4** was washed away, cells were incubated with 50 μM $NaAsO_2$ for 24 h to induce oxidative stress. Similar to SOD1(V31A), both diffusive and punctate fluorescence structures were observed in cells. The fluorescence signal was found in both cytosol and nucleus, also in consistent with SOD1(V31A).

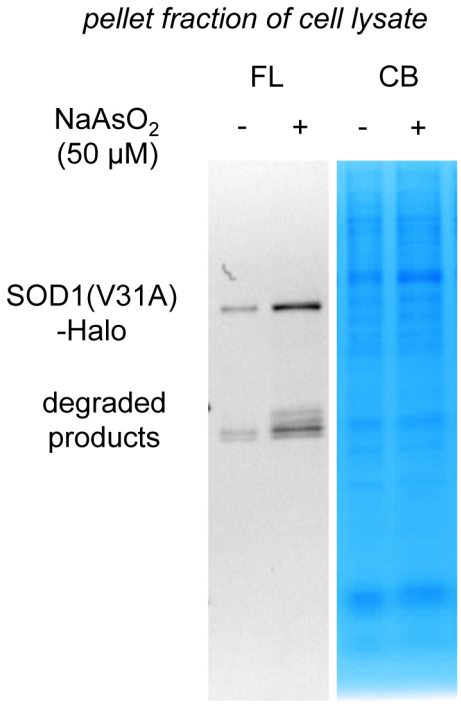

Figure S26. SOD1(V31A)-Halo fusion protein formed insoluble aggregates in cells treated with $NaAsO_2$ (extended from Figure 5b). Protein concentration of cell lysates was determined by a Bradford assay using pre-quantified BSA as a standard. Lysates of cells with or without $NaASO_2$ stress were normalized to the same concentration and centrifuged at 21,000 g for 30 min at 4 ºC. Insoluble fraction of cell lysate was resuspended in SDS-PAGE loading buffer and resolved in SDS-PAGE gel. The SOD1(V31A) was either visualized via fluorescence from **4** (FL on the right) or coomassie blue stain (CB on the right).

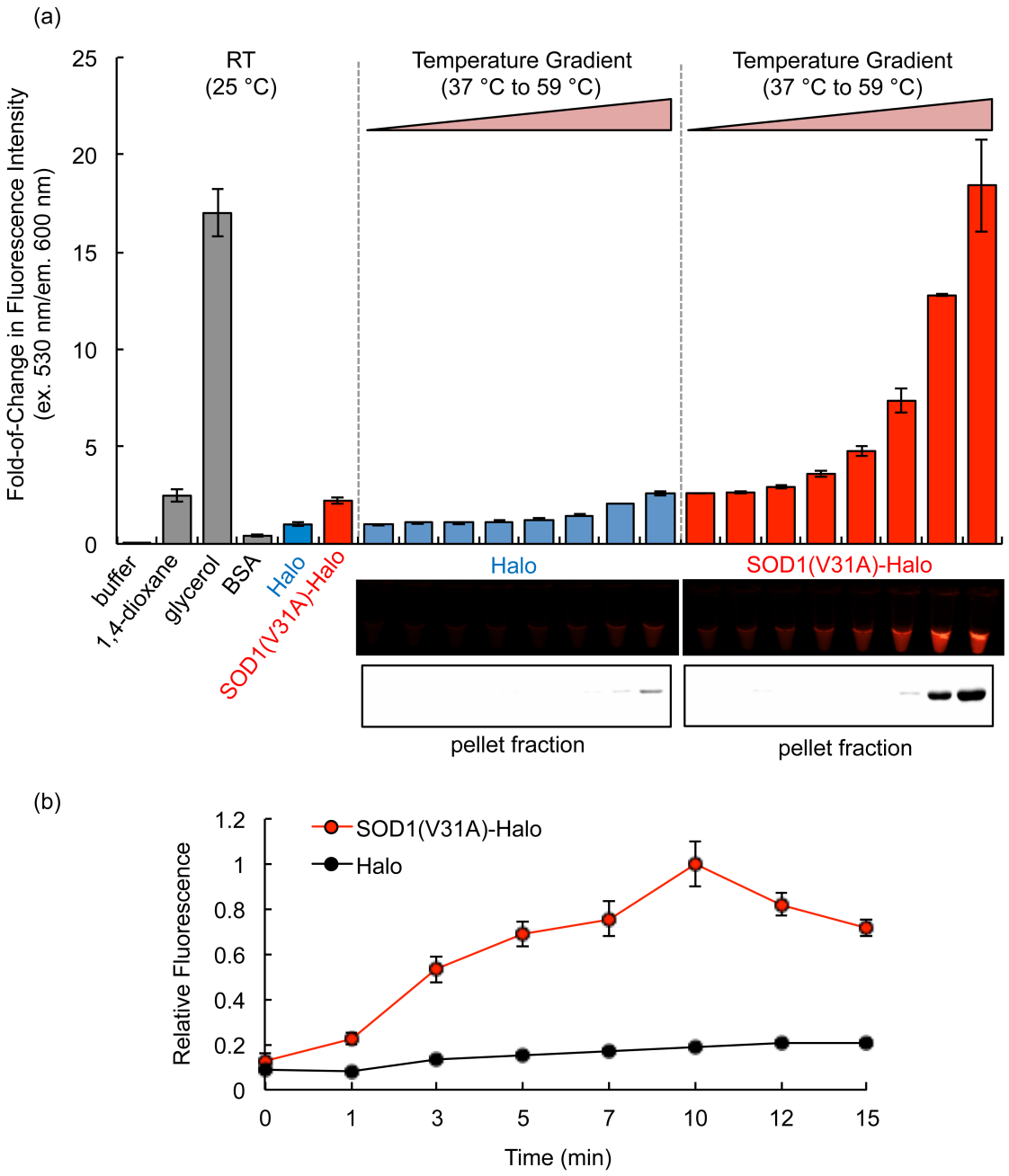

Figure S27: Purified SOD1(V31A)-Halo fusion protein formed insoluble aggregates and turned on fluorescence of 4 under heat with time and temperature dependence. (**a**) Purified SOD1(V31A)-Halo and Halo-Tag proteins (42 μM), both of which were conjugated with **4** (21 μM), were incubated at varying temperatures (25, 37, 38.9, 41.8, 45.6, 50.7, 54.5, 57.2, and 59 ºC). As control samples, **4** (21 μM) was prepared in buffer, 1,4-dioxane, glycerol, BSA (2 mg/mL). Fluorescence intensity was recorded at E_x = 530 nm/E_m = 600 nm. All readings were normalized to intensity of the Halo-Tag-**4** conjugate at 25 ºC. Fluorescence of protein samples was also visualized via UV transilluminator. In

addition, protein samples were centrifuged at 21,000 g for 30 min at 4 ºC to analyze their insoluble fraction using fluorescence of **4** as signal on SDS-PAGE gel. While obvious insoluble aggregates were only found at 57.2 and 59 ºC, turn-on fluorescence of the SOD1(V31A)-Halo-**4** conjugate was observed at lower temperatures. This data suggests that **4** is able to fluoresce prior to formation of insoluble aggregates. This fluorescence was not originated from aggregation of Halo-Tag domain, as evidenced by the low fluorescence of the Halo-**4** conjugate and lack of significant insoluble fraction at these temperatures. Error bars: standard error (n=3). (**b**) Purified SOD1(V31A)-Halo and Halo-Tag proteins (42 μM) were conjugated with **4** (21 μM) and incubated at 54.5 ºC. Fluorescence was recorded using Agilent Carey Eclipse fluorescence spectrophotometer with temperature control. Buffer condition: 50 mM Tris-HCl, pH 7.5, 100 mM NaCl, 83 mM EDTA. Parameters for fluorescence measurement: **4** (E_x = 530 nm/E_m = 600 nm).

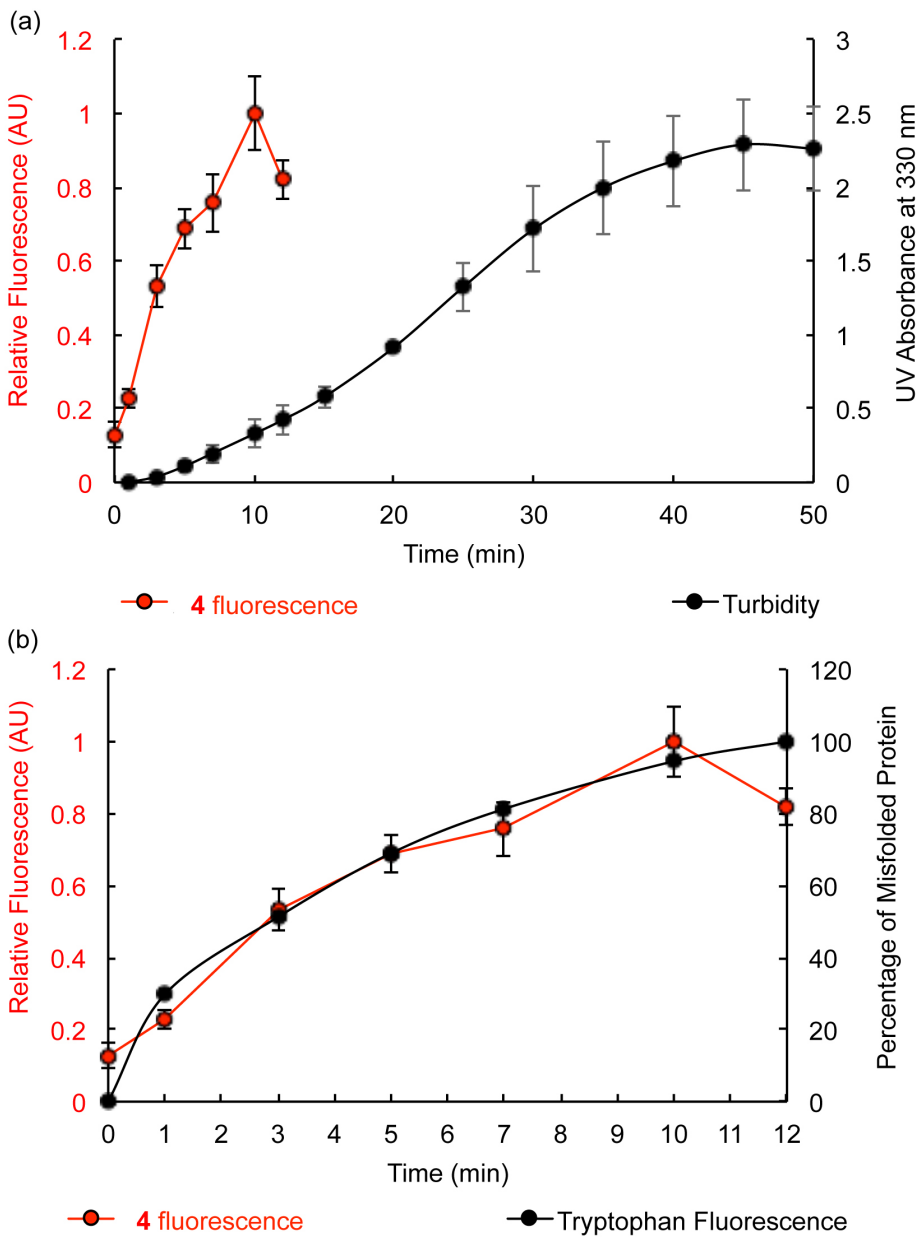

Figure S28: Fluorescence of the SOD1(V31A)-Halo•4 conjugate originates from protein misfolding. (**a**) Purified SOD1(V31A)-Halo (42 µM) was conjugated with **4** (21 µM) and incubated at 54.5 ºC. Fluorescence was recorded using Agilent Carey Eclipse fluorescence spectrophotometer with temperature control. Turbidity was recorded using Agilent 300 UV-Vis spectrophotometer. Buffer condition: 50 mM Tris-HCl, pH 7.5, 100 mM NaCl, 83 mM EDTA. (**b**) Kinetics of fluorescence increases from the SOD1(V31A)-Halo•**4** conjugate (red curve) was compared to the kinetics of protein misfolding (black curve) as measured by Tryptophan fluorescence change. Fluorescence was recorded using Agilent Carey Eclipse fluorescence spectrophotometer with temperature control. Experiments were carried out at 54.5 ºC. Parameters for fluorescence measurement: **4** (E_x = 530 nm/E_m = 600 nm) and Trp (E_x = 290 nm/E_m = 330 and 345 nm). Error bars: standard error (n=3).

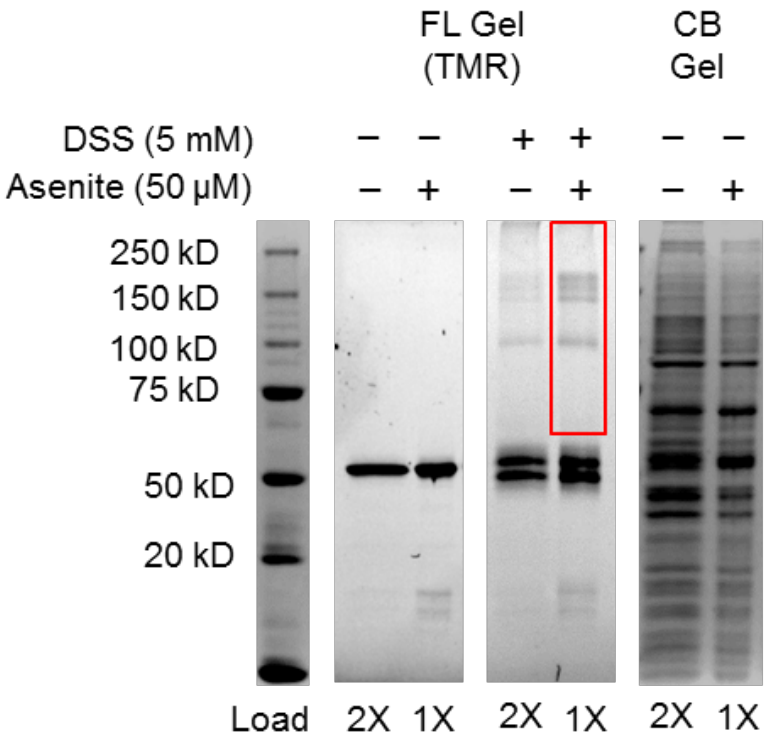

Figure S29. Chemical crosslinking experiment confirmed the presence of soluble oligomers of SOD1-V31A-Halo upon $NaAsO_2$-induced oxidative stress in HEK293T cells. Cells grown at indicated stressed conditions in 12-well culture plate were harvested and washed three times with PBS buffer (adjusted to pH 8.0). Cell density was adjusted at $2 \cdot 10^6$ cells/mL. Freshly prepared DSS (disuccinimidyl suberate, Thermo Scientific™) in DMSO was added into samples to a final concentration of 5 mM DSS and incubated at room temperature for 30 min. Crosslinking reaction were then quenched with addition of 1 M Tris buffer to a final concentration of 20 mM Tris to neutralize the reactivity of NHS ester. Cells were lysed by sonication for 1 min (20% amplitude, 1 s on, 2 s pulse). Samples were centrifuged for 30 min at 21,000 g at 4 ºC. Soluble fraction was sampled and boiled with SDS loading buffer before separated by SDS-Page gel. Lysate concentration was normalized by Bradford assay. While loading for non-stressed sample was twice as much as loading for the stressed sample, more crosslinked species at high molecular weight was identified for the stressed sample (highlighted in red box).

Table S1: The photophysical parameters of fluorophores in this work.

Compound	λ_{ex} (nm)	λ_{em} (nm)	Φ	λ_{abs} (nm)[a]	ε($M^{-1}cm^{-1}$)[a]	*B*($M^{-1}cm^{-1}$)[b]
1	370	429	0.001	376	20,592	20.6
2	450	521	0.027	452	23,717	640
3	530	630	0.221	533	39,049	8,630
3a	485	621	0.1	500	13,863	1,386
3b	530	629	0.232	530	9,004	2,089
4	530	628	0.230	534	36,241	8,335
Halo·4	530	630	0.011	533	39,049	430
SOD1(V31A)-Halo·4	530	630	0.026	533	39,049	1,015
SOD1(V31A)-Halo·4 aggregates	530	600	0.22	534	36,241	7,973

[a] Maximum absorbance and extinction coefficient measured in glycerol for small molecule probes only, and in aggregation buffer for protein samples. [b] Brightness (*B*) was calculated using $B = \Phi\varepsilon$.[1]

Table S2: The geometry of 3 extracted from crystal structure. The total energy at this geometry is -1531.67109379 Hartree.

Atom	X(Å)	Y(Å)	Z(Å)
C	8.589111	-1.881432	1.224387
H	9.139859	-1.768830	0.445329
H	8.998082	-2.518740	1.813209
H	8.497810	-1.039027	1.676078
H	7.677154	-4.210787	1.409144
C	1.255841	2.555928	-1.372002
C	2.079860	1.358102	-1.047783
C	0.014408	0.720154	-0.976268
C	3.430059	1.410384	-0.977822
H	3.804300	2.224322	-1.228115
C	4.388472	0.388601	-0.571549
C	5.727878	0.741428	-0.476613
H	5.985943	1.603805	-0.707828
C	6.346334	-1.447938	0.341371
C	4.994563	-1.813307	0.214286
H	4.734045	-2.680516	0.424980
C	4.042570	-0.906792	-0.220101
H	3.153915	-1.172817	-0.278479
C	6.889460	-3.694201	1.224295
H	6.345074	-3.645782	2.012474
H	6.392083	-4.110123	0.517262
C	-1.221120	-0.053142	-0.842227
H	-2.028992	0.350472	-1.064420

C	-1.230528	-1.321341	-0.411810
H	-0.405583	-1.688712	-0.190991
C	-2.393740	-2.195524	-0.248500
C	-2.222585	-3.502827	0.192167
H	-1.365663	-3.791036	0.412277
C	-3.271420	-4.390282	0.317704
H	-3.108393	-5.258111	0.608236
C	-4.572196	-3.996638	0.008796
C	-4.759688	-2.683641	-0.436285
H	-5.616644	-2.396456	-0.654614
C	-3.698918	-1.799250	-0.557339
H	-3.857202	-0.929174	-0.848739
H	-4.939809	-6.694154	-0.329524
C	-1.183415	2.949098	-1.368345
H	-1.934115	2.471932	-1.754659
H	-0.988762	3.709282	-1.938351
C	-1.562630	3.441717	0.009391
C	-3.264926	4.838528	1.141641
C	-2.270442	5.770712	1.793963
H	-1.500405	5.271937	2.076998
H	-2.677748	6.188832	2.556554
H	-2.003097	6.444013	1.164576
C	-3.736996	3.730646	2.074251
H	-4.412066	3.210115	1.635228
H	-4.099555	4.118614	2.875078
H	-2.995042	3.164813	2.301043

C	-4.455907	5.578691	0.551176
H	-4.145729	6.238137	-0.073121
H	-4.944598	6.008265	1.255781
H	-5.027917	4.953304	0.100110
N	1.227433	0.271319	-0.822233
N	-0.043023	2.084575	-1.330079
N	7.273613	-2.362966	0.822083
N	-5.636442	-4.884588	0.135566
O	1.575820	3.732509	-1.579503
O	-2.646351	4.215190	-0.068768
O	-0.970195	3.171377	1.011101
C	-6.986251	-4.455920	-0.216546
H	-7.206796	-3.659886	0.273176
H	-7.609525	-5.149602	0.002538
H	-7.028281	-4.273958	-1.158477
C	-5.403601	-6.297338	0.409664
H	-4.873618	-6.386220	1.205418
H	-6.246057	-6.740703	0.535678
C	6.689652	-0.155705	-0.046086
H	7.579008	0.113535	-0.016736

Table S3: The optimized ground state geometry of 3. The total energy at this geometry is -1532.25076841 Hartree.

Atom	X(Å)	Y(Å)	Z(Å)
C	-0.036826	0.932472	-1.032941
C	2.098256	1.332009	-1.005639
C	1.451146	2.595532	-1.444983
N	0.089975	2.264577	-1.451341
N	1.120481	0.368206	-0.772466
O	1.914041	3.689387	-1.751958
C	3.454159	1.222276	-0.882555
H	3.994219	2.134926	-1.129481
C	-1.333150	0.299491	-0.928217
H	-2.196780	0.905304	-1.184641
C	-1.489678	-0.989708	-0.534558
H	-0.580093	-1.538456	-0.296955
C	-0.945753	3.214075	-1.771511
H	-0.441169	4.075197	-2.226620
H	-1.649506	2.813977	-2.506158
C	-1.764693	3.747958	-0.591942
O	-2.878761	4.210626	-0.752308
O	-1.093815	3.668250	0.559227
C	-1.641331	4.181420	1.840841
C	-2.919339	3.417382	2.199771
H	-3.241093	3.708995	3.205263
H	-3.726204	3.636718	1.498878
H	-2.731510	2.338987	2.203788

C	-1.869431	5.691978	1.731937
H	-2.147865	6.085274	2.715442
H	-0.950636	6.194425	1.413320
H	-2.666797	5.926075	1.024929
C	-0.516663	3.865191	2.828606
H	-0.797716	4.202241	3.831367
H	-0.323823	2.789020	2.863759
H	0.407624	4.371841	2.536442
C	4.264270	0.096572	-0.482714
C	5.668280	0.246092	-0.432762
C	3.745878	-1.170449	-0.125004
C	6.511358	-0.788989	-0.057683
H	6.104915	1.207116	-0.693720
C	4.577244	-2.213724	0.251040
H	2.672554	-1.318037	-0.146179
C	5.988538	-2.061016	0.287948
H	7.578589	-0.607405	-0.034172
H	4.124637	-3.160373	0.519542
N	6.818086	-3.110354	0.638593
C	6.246465	-4.348922	1.145180
H	5.689058	-4.202468	2.083086
H	5.568207	-4.799964	0.411915
H	7.050363	-5.061757	1.333065
C	8.242653	-2.876765	0.820196
H	8.699298	-2.489347	-0.097802
H	8.451951	-2.165201	1.633723

H	8.731891	-3.822005	1.058483
C	-2.731073	-1.730628	-0.393322
C	-2.688844	-3.078251	0.017746
C	-4.010715	-1.186953	-0.637983
C	-3.835951	-3.845308	0.172425
H	-1.723917	-3.534800	0.224291
C	-5.166959	-1.935871	-0.489472
H	-4.109897	-0.151044	-0.948175
C	-5.116374	-3.297548	-0.087548
H	-3.732989	-4.873352	0.496285
H	-6.119017	-1.459237	-0.686739
N	-6.266293	-4.053761	0.036808
C	-7.570331	-3.418253	-0.081941
H	-7.692138	-2.944537	-1.062840
H	-8.346871	-4.177696	0.015774
H	-7.737274	-2.653653	0.691903
C	-6.191578	-5.396220	0.592838
H	-5.532005	-6.035407	-0.005561
H	-5.824940	-5.401216	1.630763
H	-7.185889	-5.843973	0.579655

Table S4: The optimized S1 excited state geometry of 3. The total energy at this geometry is -1532.24484267 Hartree.

Atom	X(Å)	Y(Å)	Z(Å)
C	-0.089657	0.994920	-1.049836
C	2.065692	1.370080	-0.989477
C	1.417330	2.643659	-1.433211
N	0.060494	2.321827	-1.454905
N	1.115816	0.423968	-0.775296
O	1.900567	3.730447	-1.730448
C	3.446838	1.281536	-0.857407
H	3.986134	2.195564	-1.092818
C	-1.335407	0.352584	-0.950384
H	-2.223718	0.922259	-1.200161
C	-1.434579	-0.979924	-0.544837
H	-0.497965	-1.482048	-0.314883
C	-0.974253	3.270482	-1.781244
H	-0.479724	4.125926	-2.255793
H	-1.683222	2.849730	-2.499034
C	-1.782098	3.814756	-0.598064
O	-2.893544	4.283860	-0.754617
O	-1.100872	3.741643	0.546958
C	-1.647138	4.240828	1.834487
C	-2.919326	3.465850	2.190346
H	-3.237101	3.743541	3.201059
H	-3.731151	3.689610	1.496618
H	-2.726110	2.388615	2.178712

C	-1.883873	5.750974	1.739360
H	-2.163514	6.133994	2.726615
H	-0.968432	6.261749	1.424081
H	-2.683399	5.986345	1.035223
C	-0.517678	3.921819	2.815942
H	-0.797282	4.248951	3.822405
H	-0.319921	2.846302	2.840984
H	0.403200	4.435829	2.525452
C	4.218807	0.146204	-0.457403
C	5.636027	0.252125	-0.380193
C	3.656890	-1.120327	-0.121087
C	6.436745	-0.807118	-0.000925
H	6.103217	1.201399	-0.629528
C	4.451978	-2.186566	0.259519
H	2.580595	-1.235073	-0.170692
C	5.866842	-2.069014	0.333851
H	7.509480	-0.662559	0.037579
H	3.970655	-3.126138	0.502977
N	6.657485	-3.131432	0.714158
C	6.054283	-4.414165	1.044933
H	5.359875	-4.326613	1.891131
H	5.503013	-4.833431	0.192443
H	6.838799	-5.118462	1.321563
C	8.104788	-2.988549	0.774858
H	8.527755	-2.731580	-0.205674
H	8.404086	-2.211878	1.491156

H	8.544715	-3.932493	1.096426
C	-2.627902	-1.747403	-0.404599
C	-2.556486	-3.104670	0.015964
C	-3.937256	-1.244714	-0.656066
C	-3.678921	-3.897402	0.169356
H	-1.579551	-3.532347	0.228963
C	-5.067241	-2.029795	-0.505640
H	-4.067774	-0.213890	-0.970090
C	-4.979276	-3.387804	-0.098200
H	-3.548598	-4.920914	0.499016
H	-6.033159	-1.582733	-0.707087
N	-6.108145	-4.184577	0.019083
C	-7.428440	-3.580047	-0.068769
H	-7.566294	-3.076096	-1.031665
H	-8.184666	-4.362872	0.004445
H	-7.611102	-2.845366	0.731849
C	-5.999834	-5.500725	0.628662
H	-5.293076	-6.131646	0.078463
H	-5.671750	-5.454590	1.679697
H	-6.973893	-5.990742	0.594547

Experimental Method Section

1. Plasmids.

Mammalian expression: pHTN vector (Promega, Inc) with a stop codon added to the c-terminal of Halo-Tag protein. The SOD-1 gene was amplified from the pF146 pSOD1WTAcGFP1 (a gift from Elizabeth Fisher, Addgene plasmid #26407), respectively. The V31A and G85R mutations were introduced to SOD1 via QuickChange PCR. The *Htt*-Q97 gene was amplified from the pCDNA3.1-*Htt*-97Q-*mCherry*, which is a generous gift from Ulric Hartl (Max Planck Institute of Biochemistry). The *Htt*-46Q was a gift from Susan Lindquist (Addgene plasmid # 1182). These genes were sub-cloned into a pHTC HaloTag CMV-neo vector by the PIPE cloning method.

Protein expression: pET29b vectors were constructed to encode Halo-Tag-His6, SOD1(V31A)-linker-Halo-His6 (linker contains a TEV protease cleavage site), SOD1-linker-Halo-His6 (linker contains a TEV protease cleavage site), and α-synuclein.

2. Protein expression and purification.

Halo-Tag and SOD1(V31A)-Halo: *E. coli* BL21 DE3* competent cells harboring a pBAD vector encoding σ32-I54N were transformed with pET29b vectors containing Halo-His6, SOD1-TEV-Halo-His6 and SOD1(V31A)-TEV-Halo-His6 proteins. Expression and purification was carried out as previously described. In brief, cells expressing recombinant proteins were thawed and lysed by sonication at 4 ºC in the presence of a protease inhibitor (1 mM PMSF). Lysed cells were centrifuged for 60 min at 16,000 × *g*. The supernatant was collected and loaded onto a 6 mL BioRad Nuvia Ni-IMAC column and washed with 120 mL of buffer containing 50 mM Tris • HCl (pH 7.5) and 100 mM NaCl. The protein

was then eluted by gradient addition of buffer containing 50 mM Tris • HCl (pH 7.5), 100 mM NaCl, and 500 mM imidazole over a volume of 48 mL. The protein fractions were identified by SDS-PAGE analysis, pooled, and concentrated. The protein was further purified using a 120 mL HiPrep^{TM} 16/60 Sephacryl^{TM} S-200 HR size-exclusion column. The protein containing fractions were identified by SDS-PAGE gel analysis, pooled, and concentrated. No significant impurities were identified and purity was estimated to be > 98% based on SDS-PAGE.

SOD1(V31A): Purified SOD1(V31A)-Halo protein was subjected to a 1 h TEV protease cleavage (0.50 μM TEV protease for every 10 μM SOD1-Halo protein) in the presence of 1 mM DTT at 25 ºC. Reaction mixture was retro-purified via BioRad Nuvia Ni-IMAC resin. Flow through was collected as cleaved SOD1(V31A). No significant impurities were identified and Halo purity was estimated to be > 98% based on SDS-PAGE.

α-synuclein: Protein expression was induced with 0.1 M IPTG, 5 hours, 37 ºC. Harvest culture at 5,000 RPM, 15 min, 4 ºC. Resuspend the pellet in DPBS (200 mg/L KCl, 200 mg/L KH_2PO_4, 8 g/L NaCl, 2.16 g/L $Na_2HPO_4•7H_2O$), transfer to a 50mL conical tube. Spin at 4,000 rpm, 30 min, 4ºC. Decant the supernatant, and store the pellet in a -80 ºC freezer. Next morning, resuspend defrosted pellet in osmotic shock buffer (30 mM Tris-HCl, 40% sucrose, 2 mM EDTA, pH 7.5; 100 mL for each liter of starter culture). Incubate for 10 min at room temperature. Collect pellet by centrifugation (12,000 rpm, 20 min). Quickly resuspend pellet with ice-cold water (90 mL for each liter of starter culture). Add 4 M $MgCl_2$ (76.5 μl for each liter of starting culture) and keep on ice for 3 min. Centrifuge at 15,000 rpm, 30 min. Collect and filter supernatant. Add 2 M Tris-HCl, pH 8 at a 1:100 (v/v) ratio. Load supernatant onto UNO Sphere Q column (5 mL, Bio-Rad), elute with a

gradient from Buffer A (20 mM Tris, pH 8) to Buffer B (20 mM Tris, 500 mM NaCl, pH 8). Analyze fractions by 15% SDS-PAGE gel. Pool protein-containing fractions, and dilute by half with degassed Buffer A. Centrifuge at 15,000 rpm, 30 min to remove aggregates. Load onto an EnrichQ column (8 mL) on the NGC-Quest10 FPLC system and elute with a gradient from 0% to 100% Buffer B. Analyze fractions by 15% SDS-PAGE gel. Pool protein-containing fractions and dilute by half with degassed Buffer A. Load onto an EnrichQ column (8 mL) and elute with a gradient from 40% to 52% Buffer B. Analyze fractions by 15% SDS-PAGE gel. Pool protein containing fractions and flash freeze small aliquots of protein. Proteins can only be thawed once before use.

3. Quantum yield measurements.

Quantum yield measurements followed the previously reported protocol [2]. Rhodamine 6G and Fluorescein were used as the quantum yield standards (QY of Rhodamine 6G is 0.95 in water and QY of Fluorescein is 0.79 in 0.1 M NaOH aqueous solution). The standard samples were prepared in water or 0.1 M NaOH. The probes (**2**, **3**, **3b** and **4**) were in DMSO as stock solutions, and prepared as 5 μM solution of 80% glycerol in ethylene glycol. A serial dilution was preformed to make a concentration gradient. Emission spectra were taken, for **2** (Ex: 450 nm) for **3**, **3a, 3b** and **4** (Ex: 490 nm) and peak area was integrated respectively to generate the quantum yields. Quantum yield of fluorophores in 100% glycerol was extrapolated via a viscosity sensitivity linear curve.

4. Confocal microscope imaging.

The HEK293T cells were seeded at 25% confluency 24 h prior to transfection in poly-D-lysine coated 35 mm glass bottom dishes (MatTek Corporation). Cells were grown in DMEM media supplemented with 10% FBS and Penicillin-Streptomycin antibiotics until

they reached 50-60% confluency. Transfection was carried out using X-tremeGene™ 9 DNA transfection reagent (Roche) according to the manufacturer's instructions. Proteins were expressed for 24 h prior to analyses. To label proteins with Halo-Tag fusion, protein expression was carried out in the presence of 1 μM **4** or 1 μM TMR Halo-Tag ligand to form covalent conjugate with the Halo-Tag domain. For a dual-probe labeling scheme, 1 μM **4** and 1 μM coumarin Halo-Tag ligand to simultaneously form covalent conjugate with the Halo-Tag domain.

To wash off unbound Halo ligands, the cells were washed extensively by replacing media with fresh DMEM and incubating for 30 min at 37 °C. For confocal fluorescence imaging with either **4**-labeled Halo fusion, TMR-labeled Halo fusion, EGFP fusion, or mCherry fusion proteins, DMEM media was replaced with FluoroBrite™ DMEM media (ThermoFisher) supplemented with 10% FBS, and Hoechst 33342 (0.1 μg/mL). For confocal fluorescence imaging with either dual-probe labeled Halo fusion with **4** and coumarin ligand, DMEM media was replaced with FluoroBrite™ DMEM media (ThermoFisher) supplemented with 10% FBS. The samples were incubated for 30 min prior to imaging. Media was replaced with fresh FluoroBrite™ DMEM media (ThermoFisher) supplemented with 10% FBS prior to imaging. Confocal images were obtained using Olympus FluoView™ FV1000 confocal microscope. The EGFP fluorescence was visualized using blue argon (488 nm) laser. Nuclear staining and coumarin fluorescence was visualized using violet laser (405 nm). Fluorescence of TMR and **4** were visualized using green HeNe laser (543 nm).

5. Chemical-induced proteome stress and confocal imaging of stressed cells.

HEK293T cultures were seeded at 25% confluency 24 h prior to transfection in 12-well plate for time dependent fluorescence plate reader analysis or 35 mm glass bottom culture dishes (Poly-*d*-lysine coated, MatTek Corporation). Cells were grown in DMEM medium supplemented with 10% FBS and penicillin-streptomycin antibiotics until they reached 50-60% confluency. Transfection was performed using X-tremeGene™ 9 DNA transfection reagent (Roche). After 24 h of protein expression and co-translational labeling, medium was replaced with fresh DMEM to diffuse out unbound ligands. After 30 min, media was replaced by fresh DMEM medium containing DMSO vehicle or $NaAsO_2$ (50 μM). Cells were incubated for 24 h, 37 ºC in a CO_2 incubator. Nuclear stain Hoechst 33342 (0.1 μg/mL) was added to the medium 30 min prior to confocal imaging.

6. Aggregation Assays.

α-synuclein: Aggregation solution contained 140 μM α-synuclein in 20 mM HEPES (pH 7.5) and 100 mM NaCl. 10 μM of **3** or ThT was added to the solution at the beginning of reaction. Previous studies have shown that the kinetics of α-synuclein aggregation is unaffected by the addition of ThT. A volume of 150 μL of the mixture was pipetted into a well of clear-bottom 96-well plate, which was subsequently sealed with Mylar plate sealers. The plate was loaded on a Heidolph vibrating platform shaker and shake at 1,350 rpm at 37 ºC. At indicated time points, fluorescence reading was obtained using a Tecan M1000Pro fluorescence plate reader. Fluorescence intensity was recorded at E_x = 530 nm/E_m = 600 nm for **3** and E_x = 450 nm/E_m = 480 nm for ThT. Each sample was run in triplicate or quadruplicate.

SOD1-Halo, SOD1(V31A)-Halo, SOD1(V31A): Aggregation was carried out with DPBS buffer containing indicated concentrations of EDTA that is used to chelate the structural metal of SOD1. Aggregation solution contained 42 μM SOD1(V31A) or SOD1(V31A)-Halo and 21 μM of **3** or **4** was added to the solution at the beginning of reaction. Reaction was carried out quiescently at indicated temperatures. Fluorescence of 3 was measured at E_x = 530 nm/E_m = 600 nm.

7. DFT/TD-DFT calculation.

Computational studies are performed using the B3LYP/6-31+G(d,p) as implemented in Gaussian Development version 16 A.03. The initial geometry of **3** is extracted from the crystal structure, and relaxed in gas phase using above method. The excited-state geometry has also been fully optimized through the time-dependent version of the same DFT method. In addition, both optimized geometries were verified as true minima on the potential energy surface via the corresponding frequency calculations. The electron density difference was calculated as the electron density at 1st excited state subtracted by that at ground state on both optimized geometries.

8. X-ray structure determination of 3.

Single crystals of **3** ($C_{28}H_{34}N_4O_3$) were grown by evaporation in EtOH and ethyl acetate mixed solvents. A suitable crystal was selected and mounted on a nylon loop, with help of paratone oil on a 'SMART APEX CCD area detector' diffractometer (molybdenum target, 1600 kW). The crystal was kept at 243 K during the data collection. Using Olex2[3], the structure was solved with the XS[4] structure solution program using Direct Methods and refined with the XL refinement package using Least Squares minimization without use of

any constraints/restraints. The hydrogen atoms were placed geometrically, and rode their parent atoms during the refinement.

Crystal Data for $C_{28}H_{34}N_4O_3$ (M = 474.59 g/mol): orthorhombic, space group $P2_12_12_1$ (no. 19), a = 9.895(4) Å, b = 21.470(10) Å, c = 25.711(12) Å, V = 5463(4) Å^3, Z = 8, T = 243 K, μ(MoKα) = 0.076 mm^{-1}, *Dcalc* = 1.154 g/cm^3, 51829 reflections measured ($3.7° \leq 2\Theta \leq 57.88°$), 13915 unique ($R_{int}$ = 0.1226, R_{sigma} = 0.1327) which were used in all calculations. The final R_1 was 0.0570 (>2sigma(I)) and wR_2 was 0.1767 (all data).

9. Negative staining electron microscopy.

Carbon-coated 400 mesh EM grids supported by Formvar film were plasma-discharged prior to use. A small amount (~ 5 μL) of sample suspension was applied onto the grids. The grids were then blotted to remove excess of the sample and stained with 1% aqueous uranyl. Images were collected at indicated resolutons.

10. Trptophan fluorescence of SOD1(V31A) was used to report on the misfolding of SOD1(V31A).

Misfolding and aggregation of SOD1(V31A) was carried out in 50 mM Tris-HCl, pH 7.5, 100 mM NaCl, 83 mM EDTA buffer. EDTA is used to chelate the structural metal of SOD1. Aggregation solution contained 42 μM SOD1(V31A)-Halo at the beginning of reaction. Reaction was carried out in a cuvette held in Agilent Cary Eclipse Fluorescence Specotrophotometer with a temperature control block at 54.5 ºC. Tryptophan fluorescence was used to determine SOD1(V31A) misfolding. Fluorescence was recorded using Agilent Carey Eclipse fluorescence spectrophotometer with temperature control. Experiments were

carried out at 54.5 ºC. Parameters for fluorescence measurement: Trp (Ex = 290 nm/Em = 330 and 345 nm).

11. Chemical crosslinking experiments.

In vitro chemical crosslinking of α-synuclein oligomers: Aggregation of α-synuclein (140 μM) was performed in low binding Eppendorf tubes with agitation (1,350 rpm) at 37 °C for 43 h in absence or presence of probe **3** (10 μM). Assay buffer is 20 mM HEPES, 100 mM NaCl at pH 7.5. Samples were taken at indicated time points and chemically crosslinked with DSS (disuccinimidyl suberate, 1.5 mM) for 30 min at room temperature according to manufacturer's instructions. 1 M Tris buffer was added to the final concentration of 20 mM to quench the crosslinking reaction for 15 min and immediately boiled with SDS loading buffer. Samples were resolved using 5% Tris-Glycine SDS-PAGE gel. To visualize the crosslinked species of higher molecular weights, the gel was stained using Pierce Silver Stain Kit (Prod # 24612). Non-crosslinked samples were resolved using 15% Tris-Glycine SDS-Page gel for loading control purpose and stained using standard coomassie blue.

In cellulo chemical crosslinking of Htt-Q46 and SOD1-V31A oligomers: Cells grown at indicated stressed conditions in 12-well culture plate were harvested and washed three times with PBS buffer (pH=8.0). Cell density was adjusted at $2 \cdot 10^6$ cells/mL. Freshly prepared DSS (disuccinimidyl suberate, Thermo Scientific™) in DMSO was added into samples to a final concentration of 5 mM DSS and incubated at room temperature for 30 min. Crosslinking reaction were then quenched with addition of 1 M Tris buffer to a final concentration of 20 mM Tris to neutralize the reactivity of NHS ester. Cells were lysed by

sonication for 1 min (20% amplitude, 1 s on, 2 s pulse). Samples were centrifuged for 30 min at 21,000 g at 4 ºC. Soluble fraction was sampled and boiled with SDS loading buffer before separated by SDS-Page gel. Lysate concentration was normalized by Bradford assay. The non-stressed sample was loaded on the gel twice more than the stressed condition but showed less crosslinked species at high-molecular weight (highlighted in red box).

12. *in vitro* competition experiment.

In this experiment, we first incubated 5 μM of purified Halo with either 5 μM of the HaloTag coumarin ligand (sample #1) or 5 μM of probe **4** (sample #2). Coumarin fluorescence was used as a signal to evaluate extent of Halo being labeled by the probe **4**. After confirming the precence of coumarin labeling in sample #1 and abscence of coumarin labeling in sample #2, we then incubated 5 μM of Halo with a mixture of 5 μM of the HaloTag coumarin ligand and 5 μM of probe **4** (sample #3). If these two ligands were able to label Halo with similar kinetics or extent ($k_{\text{coumarin}} \sim k_{\text{probe 4}}$), we should expect ~50% of the Halo to be labeled with the HaloTag coumarin ligand. Otherwise, we would expect either most of the Halo ($k_{\text{coumarin}} >> k_{\text{probe 4}}$) or very little portion of Halo ($k_{\text{coumarin}} << k_{\text{probe 4}}$) to be labeled by the HaloTag coumarin ligand. Result from sample #3 showed ~50% of Halo being labeled by the HaloTag coumarin ligand, suggesting that Halo was labeled by the HaloTag coumarin ligand and probe **4** with similar rates and to the similar extent.

13. Fractionation experiments.

Cells were lysed by sonication for 1 min at 4 ºC (20% amplitude, 1 s on, 2 s pulse). Half of the lysate was saved as the “total (T)” sample. The second half was centrifuged for 30 min at 21,000 g at 4 ºC. Soluble fraction was transferred to a new tube and labeled as

"soluble (S)". Equal volume of DPBS buffer was used to thoroughly resuspend the pellet and saved as the "insoluble (I)" fraction. These samples were either imaged as in Figure 4d or analyzed using SDS-PAGE as in Figure 5b.

14. General synthetic and chromatographic methods.

All reagents and anhydrous solvents of commercial grade were used as received unless otherwise stated. Reactions were monitored by thin layer chromatography (TLC) analysis using Silicycle® glass sheets precoated with silica gel 60 Å with detection by UV-absorption (254 nm or 365 nm). Flash column chromatography was performed using Silica Flash® F60 silica gel in the indicated solvent mixture. ^{1}H NMR and ^{13}C NMR spectra were obtained on a Bruker NMR (500/126 MHz) spectrometer in the given solvents. Chemical shifts are reported as δ-values in ppm relative to the $CDCl_3$, DMSO residual solvent peak or tetramethylsilane (TMS) as an internal standard. Coupling constants are provided in Hz. All given ^{13}C spectra are proton-decoupled. High resolution mass spectra were recorded with a Waters Q-TOF Premier quadrupole/time-offlight (TOF) mass spectrometer.

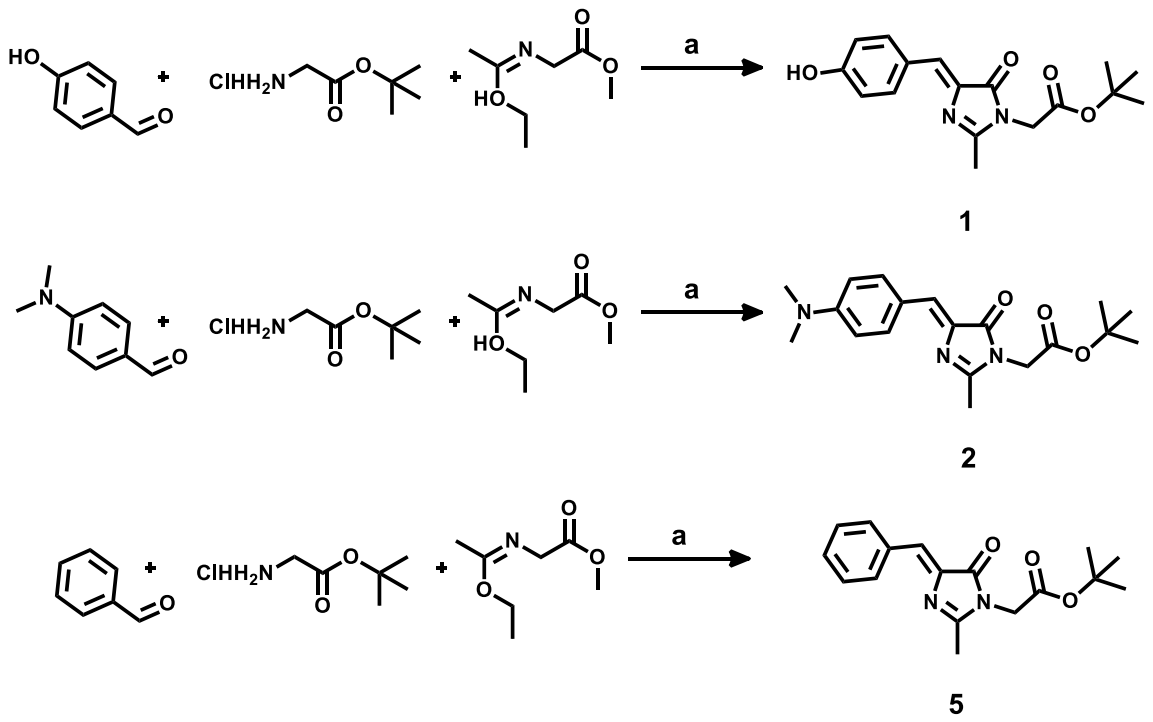

Scheme S1. Synthesis of GFP mimic precursors. Cyclization reaction to form GFP core. Condition (a) glycine *tert*-butyl ester hydrochloride (1.1 eq) was combine with NaOH (1 eq) in EtOH and stirred for 1 hour at room temperature, aldehyde (1 eq) was added and stirred overnight, imidate (1 eq) was prepared and added in one portion.[5] The reaction was stirred overnight, was then quenched by water and extracted with DCM. The organic fraction was collected and dried in vacuo. Compounds were further purified by flash chromatography (50% Ethyl Acetate, 50% Hexanes) to yield **1/2/5**.

1: (Z)-tert-butyl 2-(4-(4-(hydroxy)benzylidene)-2-methyl-5-oxo-4,5-dihydro-1H-imidazol-1-yl)acetate. Crystalline orange solid. ^{1}H NMR (500 MHz, Chloroform-*d*) δ 8.11 (d, *J* = 8.9, Hz, 2H), 6.95 (s, 1H), 6.85 (d, *J* = 8.9 Hz, 2H), 4.40 (m, 3H), 2.27 (s, 3H), 1.44 (s, 9H). ^{13}C NMR (126 MHz, Chloroform-d) δ 167.75, 161.59, 160.23, 135.95, 134.76, 126.91, 125.62, 116,27, 82.60, 42.32, 28.07, 15.53. [M+H]+ : Calcd, 317.3570, Obsd, 317.1495

2: (Z)-tert-butyl 2-(4-(4-(dimethylamino)benzylidene)-2-methyl-5-oxo-4,5-dihydro-1H-imidazol-1-yl)acetate. Crystalline orange solid. ^{1}H NMR (500 MHz, Chloroform-*d*) δ 8.07 (d, *J* = 8.9 Hz, 2H), 7.11 (s, 1H), 6.70 (d, *J* = 8.8 Hz, 2H), 4.29 (s, 2H), 3.05 (s, 6H), 2.31 (s, 3H), 1.48 (s, 9H). ^{13}C NMR (126 MHz, Chloroform-d) δ 170.11, 166.90, 158.03, 151.56, 134.27, 134.22, 129.41, 122.19, 111.72, 82.83, 42.15, 40.04, 27.99, 15.43. [M+H]+ : Calcd, 344.1896, Obsd, 344.1983

5: (Z)-tert-butyl 2-(4-benzylidene-2-methyl-5-oxo-4,5-dihydro-1H-imidazol-1-yl)acetate. Crystalline yellow solid. ^{1}H NMR (500 MHz, Chloroform-*d*) δ 8.05 (d, *J* = 8.8, Hz, 2H), 7.30 (m, 3H), 7.01 (s, 1H), 4.19 (s, 2H), 2.23 (s, 3H), 1.39 (s, 9H). [M+H]+ : Calcd, 301.3580, Obsd, 301.3367

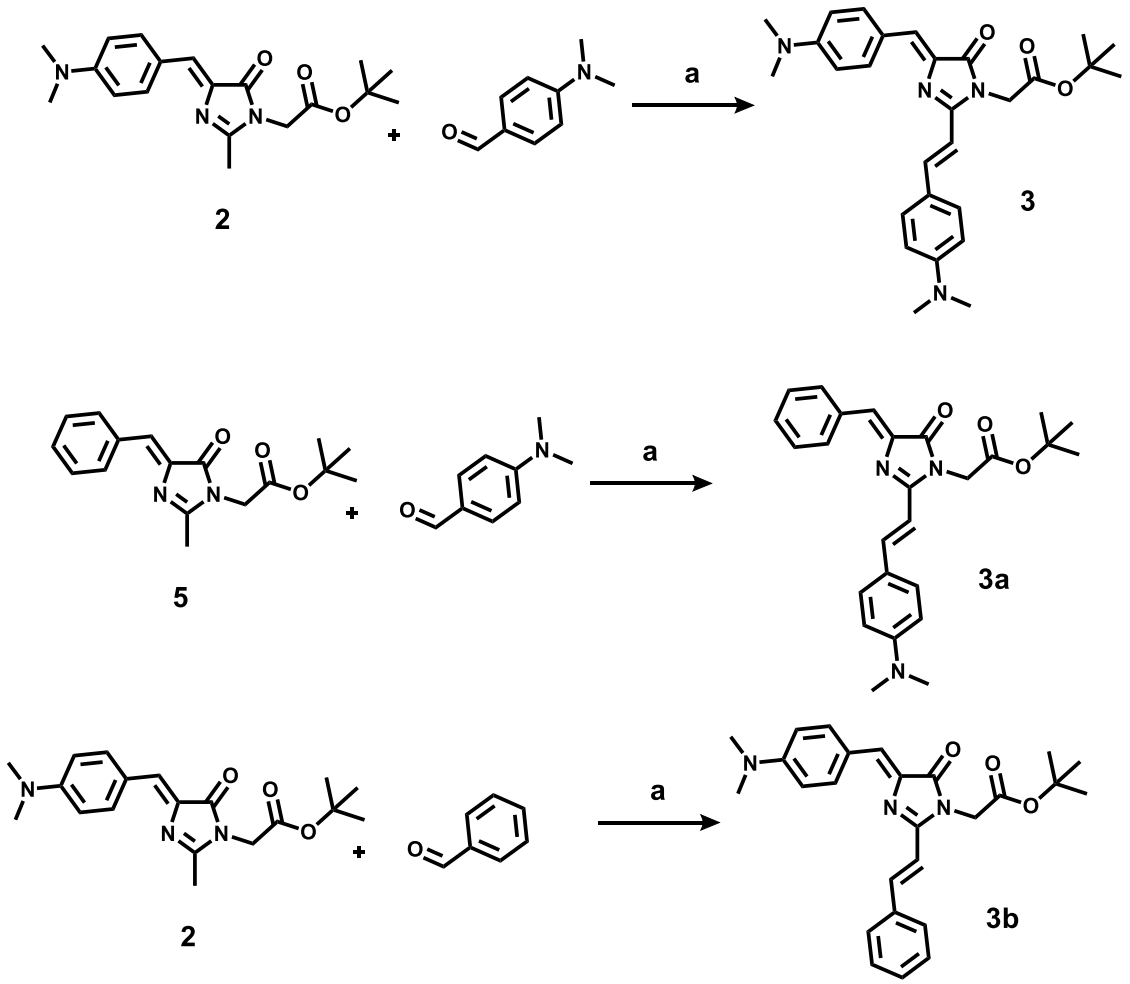

Scheme S2. General protocol for synthesis of *in vitro* GFP mimic probe. Carbon-carbon double bond formation via aldol condensation. Conditions, aldehyde (2eq), **2** or **5** (1 eq) were combine in dioxane under Argon. $ZnCl_2$ (0.01 eq) was added and the reaction was refluxed overnight. Solvent was removed and compounds were purified by flash chromatography (2:5, EA:Hexanes) to yield final GFP mimic probes **3/3a/3b**.

3: tert-butyl 2-((Z)-4-(4-(dimethylamino)benzylidene)-2-((E)-4-(dimethylamino)styryl)-5-oxo-4,5-dihydro-1H-imidazol-1-yl)acetate. Red Solid. ^{1}H NMR (500 MHz, Chloroform-^{d}) δ 8.19 (d, J = 8.6 Hz, 2H), 7.97 (d, J = 15.6 Hz, 1H), 7.48 (d, J = 8.7, 2H), 6.75 (d, J = 8.6 , 2H), 6.70 (d, J = 8.6, 2H), 6.42 (d, J = 15.6 Hz, 1H), 4.45

(s, 2H), 3.07 (d, J = 15.1 Hz, 12H), 1.49 (m, 9H). ^{13}C NMR (126 MHz, Chloroform-*d*) δ 170.36, 167.11, 156.60, 151.43, 151.34, 149.45, 139.93, 135.54, 134.83, 134.30, 132.48, 129.40, 129.17, 127.63, 123.53, 123.21, 112.91, 111.95, 111.85, 111.71, 107.58, 82.72, 60.39, 42.79, 42.37, 40.17, 40.11, 40.03, 31.24, 29.71, 28.03, 27.98, 21.06, 14.21. [M+H]+ Calcd, 475.2664, Obsd, 475.3517

3a: tert-butyl 2-((Z)-4-benzylidene-2-((E)-4-(dimethylamino)styryl)-5-oxo-4,5-dihydro-1H-imidazol-1-yl)acetate. Red oil. ^{1}H NMR (500 MHz, Chloroform-*d*) δ 8.25 (d, J = 8.5, 2H), 8.15 (d, J = 15.6 1H), 7.56 – 7.50 (m, 2H), 7.46 (t, J = 7.6 Hz, 2H), 7.41 – 7.37 (m, 1H), 7.12 (s, 1H), 6.75 (d, J = 8.6, 2H), 6.41 (d, J = 15.5 Hz, 1H), 4.46 (d, J = 8.8 Hz, 2H), 3.07 (s, 6H), 1.50 (s, 9H). ^{13}C NMR (126 MHz, Chloroform-*d*) δ 171.14, 170.53, 166.78, 159.80, 151.79, 142.13, 139.38, 134.98, 132.96, 132.37, 132.31, 132.18, 129.88, 129.67, 129.62, 128.64, 128.56, 125.54, 123.02, 111.89, 110.99, 106.56, 82.98, 60.39, 42.34, 40.13, 34.67, 34.53, 31.65, 31.59, 29.71, 29.06, 28.00, 27.96, 25.28, 22.66, 21.10, 21.05, 20.70, 14.20, 14.12, 11.43. [M+H]+ Calcd, 432.2242, Obsd, 432.2269

3b: tert-butyl 2-((Z)-4-(4-(dimethylamino)benzylidene)-5-oxo-2-((E)-styryl)-4,5-dihydro-1H-imidazol-1-yl)acetate. Red solid. ^{1}H NMR (500 MHz, Chloroform-d) δ 8.20 (d, J = 8.7 Hz, 2H), 8.01 (d, J = 15.8 Hz, 1H), 7.65 – 7.57 (m, 2H), 7.42 (tt, J = 8.5, 4.1 Hz, 3H), 7.20 (s, 1H), 6.80 (d, J=8.7, 2H), 6.68 (d, J = 15.8 Hz, 1H), 4.47 (s, 2H), 3.10 (s, 6H), 1.48 (s, 9H). ^{13}C NMR (126 MHz, Chloroform-d) δ 170.11, 166.99, 155.57, 151.68, 139.12, 135.56, 135.04, 134.71, 129.72, 129.70, 128.94, 127.67, 122.82, 113.34, 111.84, 82.92, 67.10, 42.33, 40.10, 29.72, 27.98.

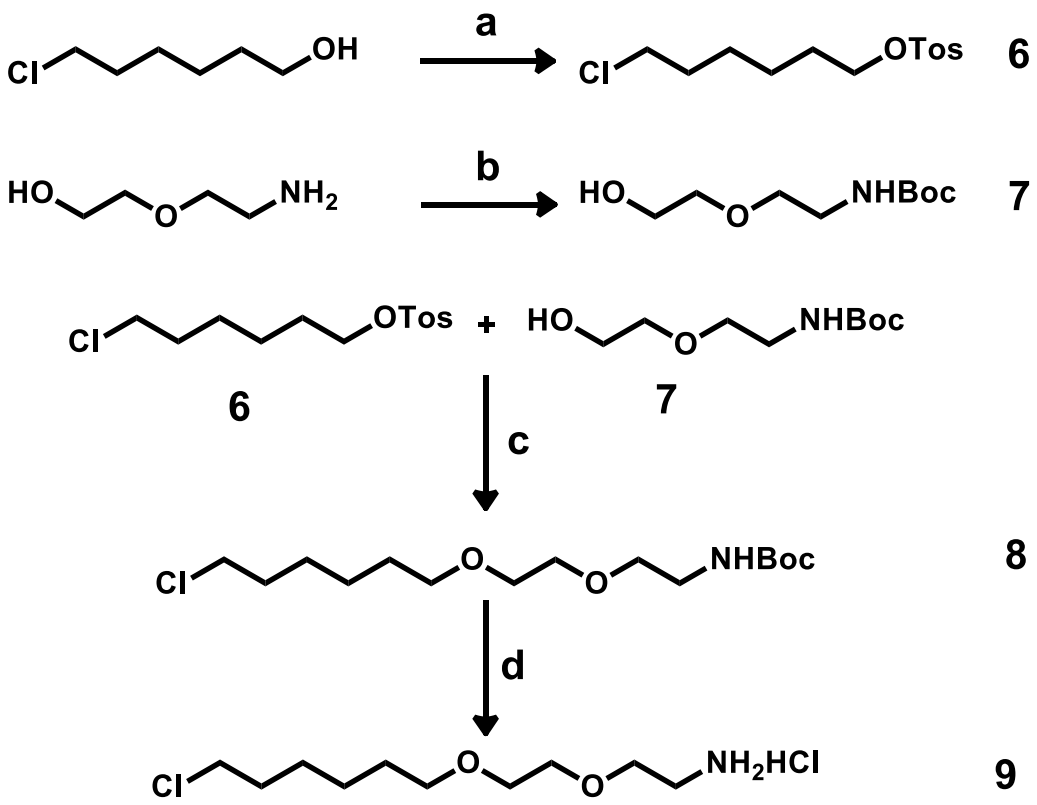

Scheme S3. Synthesis of PEG linker in large scale. Commercially available chloro-alcohol was converted into tosylate. Condition (a) 6-Chloro-1-hexanol (1.0 eq.), p-Toluenesulfonyl chloride (1.1 eq), 4-dimethylaminopyridine (0.1 eq) in pyridine for 1.5 hours at 0°C. The reaction mixture was extracted with diethyl ether against diluted HCl. The organic phase was collected and evaporated under reduced pressure, yielding crude colorless crystal **6**. The product was carried on to the next step without further purification. Commercially available amino-alcohol was protected with t-butyl carbonate group. Condition (b) 2-(2-Aminoethoxy)ethanol (1.0 eq.), Di-tert-butyl dicarbonate (1.0 eq.) in methanol stirred for 3 h at room temperature. The reaction mixture was extracted with PBS Buffer against dichloromethane. The organic fraction was dried in vacuo. Compounds were further purified by flash chromatography (1:1 ethyl acetate/hexane) to yield **7**, a colorless

oil. **6** and **7** were combined to become protected PEG linker. Condition (c) **6** (1 eq), **7** (1.1 eq), and Potassium tert-butoxide (1 M in THF, 1.5 eq) in DMF stirred overnight at room temperature. The reaction was quenched with water and extracted with diethyl ether. The product was further purified by flash chromatography (1:2 ethyl acetate: hexane). Colorless oil **8** was obtained. Deprotection of **8** yielded the PEG amine hydrochloride. Condition (d) **8** (1 eq), HCl (4 M in Dioxane, 6 eq) stirred for 1 h at room temperature. Concentrated and then dried under high-vac to yield **9** a white solid.

6: 6-chlorohexyl 4-methylbenzenesulfonate. Colorless Crystal. (R_f=0.55, 1:9 EA:Hexane). ^{1}H NMR (500 MHz, $CDCl_3$) δ 7.73 (d, *J* = 8.3 Hz, 2H), 7.31 (d, *J* = 8.4 Hz, 2H), 3.97 (t, *J* = 6.4 Hz, 2H), 3.43 (t, *J* = 6.6 Hz, 2H), 2.39 (s, 3H), 1.73 – 1.54 (m, 4H), 1.39 – 1.24 (m, 4H). ^{13}C NMR (126 MHz, $CDCl_3$) δ 144.73, 132.99, 129.81, 127.73, 70.37, 44.75, 32.19, 28.54, 26.05, 24.57, 21.51. $[M+Na]^+$: Calcd, 313.0641, Obsd, 313.0639.

7: tert-butyl (2-(2-hydroxyethoxy)ethyl)carbamate. Colorless oil. ^{1}H NMR (500 MHz, $CDCl_3$) δ 5.29 (s, 1H), 3.73 – 3.64 (m, 2H), 3.56 – 3.45 (m, 4H), 3.31 – 3.15 (m, 3H), 1.45 – 1.34 (m, 9H). ^{13}C NMR (126 MHz, CDCl3) δ 156.26, 79.30, 72.32, 70.31, 61.55, 40.37, 28.42. HRMS for $[M+Na]^+$: Calcd, 228.1212, Obsd, 228.1220.

8: tert-butyl (2-(2-((6-chlorohexyl)oxy)ethoxy)ethyl)carbamate. Colorless oil. ^{1}H NMR (500 MHz, $CDCl_3$) δ 5.02 (s, 1H), 3.58 – 3.47 (m, 8H), 3.42 (t, *J* = 6.6 Hz, 2H), 3.30 – 3.24 (m, 2H), 1.78 – 1.70 (m, 2H), 1.60 – 1.53 (m, 2H), 1.46 – 1.38 (m, 11H), 1.38 – 1.30 (m, 2H). ^{13}C NMR (126 MHz, $CDCl_3$) δ 156.03, 79.12, 71.28, 70.28, 70.22, 70.06, 45.02, 40.37, 32.56, 29.46, 28.44, 26.70, 25.44. $[M+Na]^+$: Calcd, 346.1761, Obsd, 346.1765.

9: 2-(2-((6-chlorohexyl)oxy)ethoxy)ethanamine hydrochloride. White solid. ^{1}H NMR (500 MHz, DMSO) δ 8.26 (s, 3H), 3.65 – 3.58 (m, 4H), 3.56 – 3.52 (m, 2H), 3.51 – 3.46

(m, 2H), 3.36 (t, J = 6.6 Hz, 2H), 2.94 – 2.87 (m, 2H), 1.73 – 1.65 (m, 2H), 1.51 – 1.44 (m, 2H), 1.41 – 1.33 (m, 2H), 1.33 – 1.25 (m, 2H). ^{13}C NMR (126 MHz, DMSO) δ 70.23, 69.70, 69.34, 66.58, 45.39, 38.37, 32.03, 29.06, 26.13, 24.93. $[M+H]^+$: Calcd, 224.1417, Obsd, 224.1411.

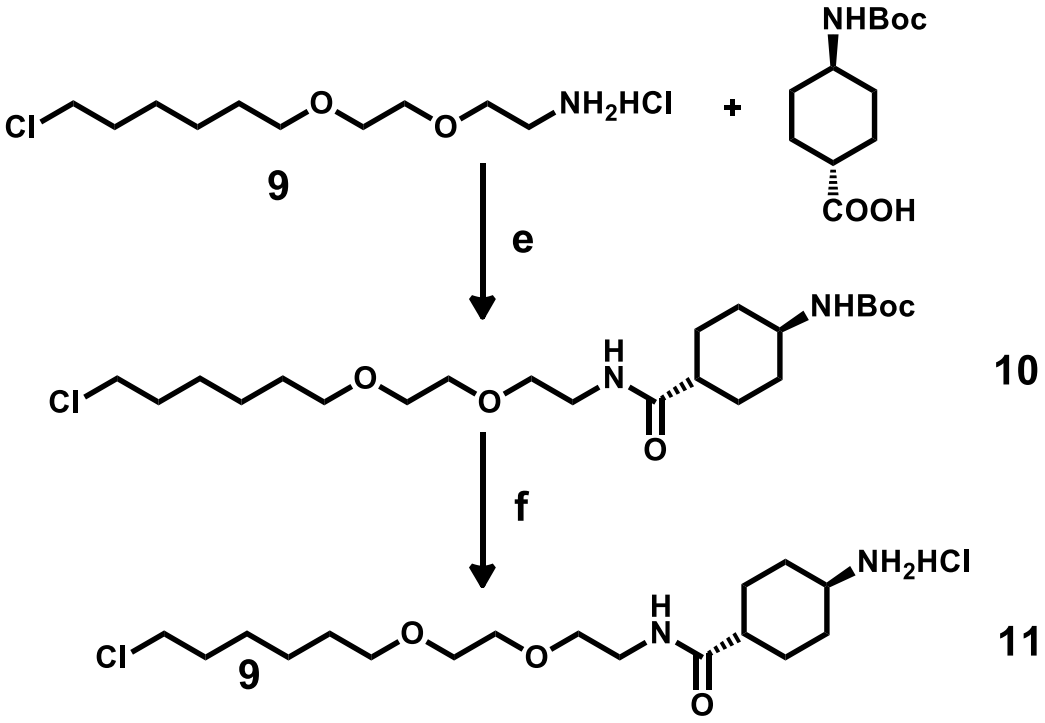

Scheme S4. Synthesis of rigid linker for small molecule probe. Commercially available cyclohexane linker was coupled with homemade PEG linker. Condition (e) **9** (1 eq.), trans-4-[[(1,1-Dimethylethoxy)carbonyl]amino]cyclohexanecarboxylic acid (1 eq.), dimethylaminopyridine (0.1 eq.), N-(3-Dimethylaminopropyl)-N'-ethylcarbodiimide hydrochloride (2 eq.) in triethylamine (4 eq.) stirred overnight at room temperature. The reaction mixture was quenched by water and extracted with DCM. Product was purified by flash chromatography (100% ethyl acetate). Sticky white solid **10** was obtained. Deprotection was of **10** yields final rigid linker amine hydrochloride. Condition (f) **10** (1 eq.), in HCl (4 M in Dioxane, 6 eq.) for 1h at room temperature. Reaction was concentrated and put under high-vac to yield fluffy white solid **11**.

10: tert-butyl ((1r,4r)-4-((2-(2-((6-chlorohexyl)oxy)ethoxy)ethyl)carbamoyl)cyclohexyl)carbamate. Sticky white solid**.**

^{1}H NMR (500 MHz, $CDCl_3$) δ 5.99 (s, 1H), 4.45 – 4.38 (m, 1H), 3.61 – 3.49 (m, 8H), 3.47 – 3.37 (m, 5H), 2.10 – 2.03 (m, 2H), 2.01 – 1.95 (m, 1H), 1.93 – 1.85 (m, 2H), 1.79 – 1.71 (m, 2H), 1.62 – 1.51 (m, 4H), 1.47 – 1.40 (m, 11H), 1.39 – 1.32 (m, 2H), 1.13 – 1.03 (m, 2H). ^{13}C NMR (126 MHz, $CDCl_3$) δ 175.29, 155.23, 79.23, 71.32, 70.30, 70.07, 69.86, 49.13, 45.10, 44.63, 39.06, 32.80, 32.58, 29.54, 28.49, 26.75, 25.48. $[M+H]^+$: Calcd, 449.2782, Obsd, 449.2783.

11: (1r,4r)-4-amino-N-(2-(2-((6-chlorohexyl)oxy)ethoxy)ethyl)cyclohexanecarboxamide hydrochloride. Fluffy white solid. ^{1}H NMR (500 MHz, DMSO) δ 8.19 (s, 3H), 7.87 (s, 1H), 3.61 (t, J = 6.6 Hz, 2H), 3.52 – 3.43 (m, 4H), 3.40 – 3.33 (m, 4H), 3.20 – 3.13 (s, 2H), 2.96 – 2.87 (m, 1H), 2.11 – 2.03 (m, 1H), 2.01 – 1.94 (m, 2H), 1.78 – 1.65 (m, 4H), 1.53 – 1.43 (m, 2H), 1.43 – 1.25 (m, 8H). ^{13}C NMR (126 MHz, DMSO) δ 174.43, 70.18, 69.59, 69.45, 69.07, 48.75, 45.39, 42.46, 38.39, 32.03, 29.43, 29.07, 27.19, 26.12, 24.94. $[M+H]^+$: Calcd, 349.2258, Obsd, 349.2257.

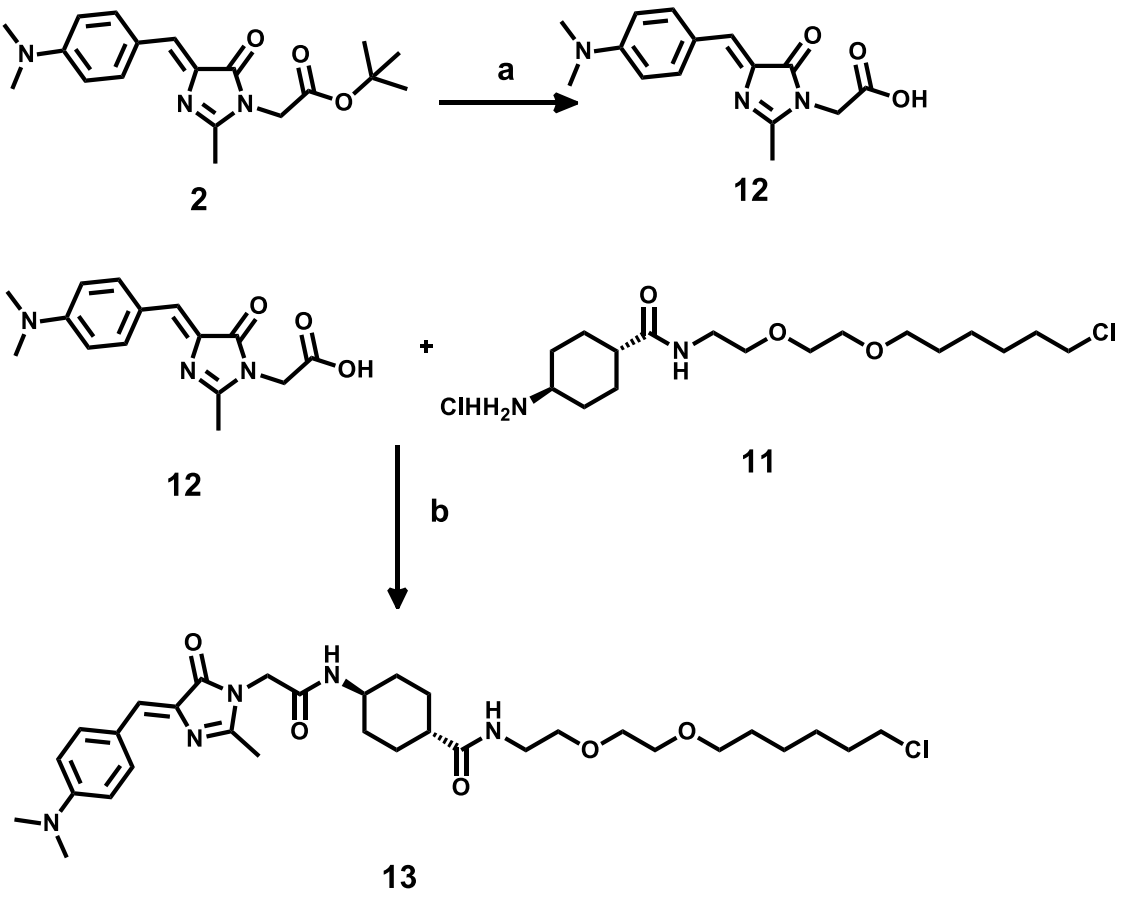

Scheme S5. Synthesis of GFP mimic precursors with rigid Halo linker. Deprotection of GFP core. Condition (a) **2** deprotected according to literature protocols to yield **12** which was used without further purification. GFP core was coupled with rigid Halo linker. Condition (b) **2** (1 eq), **11** (1.0 eq), dimethylaminopyridine (0.1 eq), N-(3-Dimethylaminopropyl)-N'-ethylcarbodiimide hydrochloride (2.0 eq), triethylamine (4.0 eq), overnight, RT. The reaction mixture was quenched by water and extracted with DCM. The organic fraction was collected and dried in vacuo. Compounds were further purified by flash chromatography (20:1, DCM:MeOH) to yield **13** a yellow powder.

13: (1r,4r)-N-(2-(2-((6-chlorohexyl)oxy)ethoxy)ethyl)-4-(2-((Z)-4-(4-(dimethylamino)benzylidene)-2-methyl-5-oxo-4,5-dihydro-1H-imidazol-1-

yl)acetamido)cyclohexanecarboxamide. Yellow powder. ^{1}H NMR (500 MHz, Chloroform-*d*) δ 8.09 (d, *J* = 8.8 Hz, 2H), 7.14 (s, 1H), 6.73 (d, *J* = 8.9 Hz, 2H), 6.17 – 5.87 (m, 2H), 4.23 (s, 2H), 3.60 – 3.40 (m, 10H), 3.09 (s, 6H), 2.40 (s, 3H), 2.10 –1.32 (m, 18H), 1.22 – 1.09 (m, 2H). ^{13}C NMR (126 MHz, Chloroform-d) δ 174.99, 170.56, 166.29, 157.54, 151.88, 134.58, 133.55, 130.56, 121.83, 111.76, 71.26, 70.24, 69.99, 69.80, 48.20, 45.07, 44.76, 44.36, 40.05, 39.01, 32.51, 32.03, 29.45, 28.25, 26.68, 25.40, 15.59. [M+H]+ : Calcd, 618.3344, Obsd, 618.3441.

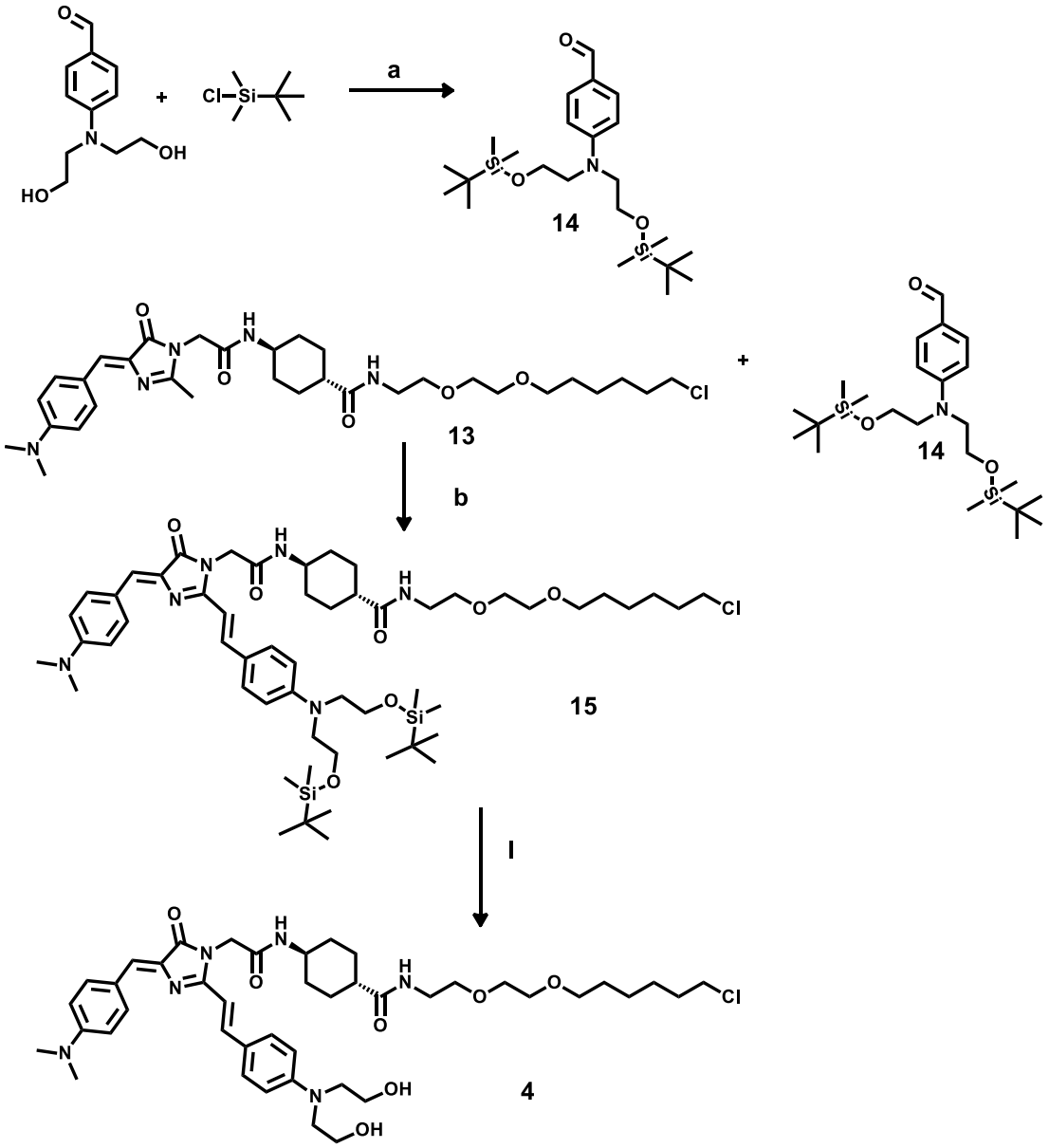

Scheme S6. Protocol for synthesis of *in vivo* GFP mimic probe. TBDMS protection. Conditions (a) 4-[Bis(2-hydroxyethyl)amino]benzaldehyde (1.0 eq) and imidazole (4.2 eq) were combined in DMF at room temperature, chloro(1,1-dimethylethyl)dimethylsilane (2.2 eq) was added and stirred for 1.5 hours. The reaction mixture was quenched with 1M HCl and extracted with ether. The organic fraction was collected and dried in vacuo to yield **14** a transparent brown oil, product was used without further purification. Carbon-carbon double bond formation via aldol condensation. Conditions (b) **14** (2.0 eq), **13** (1.0

eq) were combine in in dioxane under Argon. $ZnCl_2$ (0.01 eq) was added and the reaction was refluxed overnight. Solvent was removed and compounds were purified by flash chromatography (20:1, DCM:MeOH) to yield **15**. Product was immediately deprotected. Conditions (l) **15** (1.0 eq) was combined with TBAF (3.0 eq) in THF and stirred overnight. Compounds were purified by flash chromatography (10:1, DCM:MeOH) to yield **4** a pink solid.

4: (1r,4r)-4-(2-((Z)-2-((E)-4-(bis(2-hydroxyethyl)amino)styryl)-4-(4-(dimethylamino)benzylidene)-5-oxo-4,5-dihydro-1H-imidazol-1-yl)acetamido)-N-(2-(2-((6-chlorohexyl)oxy)ethoxy)ethyl)cyclohexanecarboxamide. Pink solid. ^{1}H NMR (500 MHz, DMSO-d6) δ 8.17 (d, J = 8.3 Hz, 2H), 7.79 (d, J = 15.5 Hz, 1H), 7.55 (d, J = 8.7 Hz, 2H), 6.84 (s, 1H), 6.80 (dd, J = 9.9, 2.7 Hz, 2H), 6.75 (dd, J = 8.6, 5.5 Hz, 2H), 6.66 (d, J = 15.5 Hz, 1H), 4.82 (s, 2H), 4.38 (s, 2H), 3.59 – 3.43 (m, 12H), 3.41 – 3.35 (m, 6H), 3.20-3.13 (m, 2H) 3.04 (s, 6H), 2.12 – 1.17 (m, 18H). ^{13}C NMR (126 MHz, DMSO-d6) δ 175.24, 170.22, 166.39, 158.07, 151.49, 150.02, 139.33, 135.98, 134.26, 130.23, 125.20, 122.97, 122.84, 112.28, 111.89, 111.42, 108.29, 70.64, 70.04, 69.90, 69.55, 58.67, 58.60, 58.43, 53.59, 49.07, 48.09, 45.83, 43.53, 42.65, 38.85, 32.48, 32.07, 29.54, 28.61, 26.59, 25.40, 13.99. [M+H]+ Calcd, 809.4357, Obsd, 809.4369.

Supplementary References:

1. Kalaparthi, V.; Palantavida, S.; Sokolov, I., The nature of ultrabrightness of nanoporous fluorescent particles with physically encapsulated fluorescent dyes. *J Mater Chem C* **2016,** *4* (11), 2197-2210.
2. Wurth, C.; Grabolle, M.; Pauli, J.; Spieles, M.; Resch-Genger, U., Relative and absolute determination of fluorescence quantum yields of transparent samples. *Nat Protoc* **2013,** *8* (8), 1535-1550.
3. Dolomanov, O. V.; Bourhis, L. J.; Gildea, R. J.; Howard, J. A. K.; Puschmann, H., OLEX2: a complete structure solution, refinement and analysis program. *J Appl Crystallogr* **2009,** *42*, 339-341.
4. Sheldrick, G. M., A short history of SHELX. *Acta Crystallogr A* **2008,** *64*, 112-122.
5. Baldridge A., Kowalik J., Tolbert L. M., Efficient synthesis of new 4-arylideneimidazolin-5-ones related to the GFP chromophore by 2+3 cyclocondensation of arylideneimines with imidate ylides, *Synthesis* **2010**, 14, 2424-2436.